JOURNAL OF BACTERIOLOGY, June 2009, p. 3950–3964 Vol. 191, No. 12
0021-9193/09/$08.00+0 doi:10.1128/JB.00016-09

Development of a *mariner*-Based Transposon and Identification of *Listeria monocytogenes* Determinants, Including the Peptidyl-Prolyl Isomerase PrsA2, That Contribute to Its Hemolytic Phenotype▽

Jason Zemansky,[1] Benjamin C. Kline,[1] Joshua J. Woodward,[1] Jess H. Leber,[1]† Hélène Marquis,[3] and Daniel A. Portnoy[1,2]*

Department of Molecular and Cellular Biology[1] and School of Public Health,[2] University of California, Berkeley, California 94720-3202, and Department of Microbiology and Immunology, Cornell University, Ithaca, New York 14853[3]

Received 6 January 2009/Accepted 6 April 2009

Listeriolysin O (LLO) is a pore-forming toxin that mediates phagosomal escape and cell-to-cell spread of the intracellular pathogen *Listeria monocytogenes*. In order to identify factors that control the production, activity, or secretion of this essential virulence factor, we constructed a *Himar1 mariner* transposon delivery system and screened 50,000 mutants for a hypohemolytic phenotype on blood agar plates. Approximately 200 hypohemolytic mutants were identified, and the 51 most prominent mutants were screened ex vivo for intracellular growth defects. Eight mutants with a phenotype were identified, and they contained insertions in the following genes: lmo0964 (similar to *yjbH*), lmo1268 (*clpX*), lmo1401 (similar to *ymdB*), lmo1575 (similar to *ytqI*), lmo1695 (*mprF*), lmo1821 (similar to *prpC*), lmo2219 (*prsA2*), and lmo2460 (similar to *cggR*). Some of these genes are involved in previously unexplored areas of research with *L. monocytogenes*: the genes *yjbH* and *clpX* regulate the disulfide stress response in *Bacillus subtilis*, and the *prpC* phosphatase has been implicated in virulence in other gram-positive pathogens. Here we demonstrate that *prsA2*, an extracytoplasmic peptidyl-prolyl *cis*/*trans* isomerase, is critical for virulence and contributes to the folding of LLO and to the activity of another virulence factor, the broad-range phospholipase C (PC-PLC). Furthermore, although it has been shown that *prsA2* expression is linked to PrfA, the master virulence transcription factor in *L. monocytogenes* pathogenesis, we demonstrate that *prsA2* is not directly controlled by PrfA. Finally, we show that PrsA2 is involved in flagellum-based motility, indicating that this factor likely serves a broad physiological role.

Listeria monocytogenes is a gram-positive, facultative intracellular pathogen capable of infecting a broad range of animal hosts, including humans (84). The cell biology of infection has been well characterized and is a model for pathogenesis. Upon internalization into host cells, including macrophages and nonprofessional phagocytes, *L. monocytogenes* organisms are initially enclosed in a single-membrane vacuole. Bacteria rapidly lyse this primary vacuole and replicate in the cytosol, exploiting actin-based motility as a means to move within the cytoplasm and to spread from cell to cell. Actin-based propulsion of bacteria from the cytoplasm of one cell into the cytoplasm of a neighboring cell results in the formation of a double-membrane vacuole or secondary vacuole. Bacteria lyse the secondary vacuole, and intracellular growth continues (81, 84).

Central to the virulence of *L. monocytogenes* is the ability to lyse the primary and secondary vacuoles in order to gain entry into the host cytosol. Escape from both types of vacuoles is primarily mediated by the secretion of the cytolysin listeriolysin O (LLO) (68). Members of a large family of pore-forming toxins called the cholesterol-dependent cytolysins, LLO monomers bind cholesterol-containing host membranes. Upon binding, the monomers oligomerize and the resultant complex inserts into the membrane, producing pores up to 30 nm in diameter (1, 68). Bacteria deficient for LLO production or activity remain trapped within a phagosome (17, 68) and are unable to replicate in cells, resulting in a 5-log decrease in virulence in mice compared to the virulence of wild-type (WT) bacteria (12, 36, 57).

However, LLO activity must be compartmentalized to the acidic phagosome. Unrestricted activity can lead to premature host cell lysis, exposing the bacteria to the inhospitable extracellular environment (22, 33). Mutants incapable of restricting the activity of LLO to the vacuole have been isolated and are up to 4 orders of magnitude less virulent in vivo than WT bacteria (13, 22, 23, 45, 46). LLO is therefore regulated at multiple levels.

Expression of *hly*, the gene encoding LLO, is controlled by the *L. monocytogenes* master virulence transcriptional activator PrfA (24, 71). In addition to *hly*, PrfA coordinately regulates the expression of several other genes necessary for *L. monocytogenes* pathogenesis, such as the broad-range phospholipase C (PC-PLC). Although a dramatic change in the expression profile of bacteria occurs during the transition into the infectious life cycle, only 10 genes (including *hly*) have been demonstrated to be directly regulated by PrfA (7, 24, 71). An unexplored possibility, therefore, remains that LLO production, activity, or secretion is regulated by other extragenic factors.

Transposon mutagenesis remains one of the most important

* Corresponding author. Mailing address: Department of Molecular & Cell Biology, 510 Barker Hall no. 3202, University of California, Berkeley, Berkeley, CA 94720-3202. Phone: (510) 643-3926. Fax: (510) 643-6334. E-mail: portnoy@berkeley.edu.

† Present address: Department of Microbiology, University of Chicago, Chicago, IL 60637.

▽ Published ahead of print on 17 April 2009.

tools in bacterial genetics, facilitating the discovery and exploration of gene function and protein interaction. Given that transposon mutagenesis has previously proved to be an effective tool in analyzing hemolysin mutants of *L. monocytogenes* (18, 36, 57), we constructed a *Himar1 mariner*-based transposon and performed a sheep's blood agar screen for mutants with a hypohemolytic phenotype. We hypothesized that transposon insertion mutants deficient in the production of LLO would reveal either novel virulence factors or additional roles for known factors. To our knowledge, there has never been a published screen that sought to characterize mutants with hypohemolytic phenotypes.

Isolated from the horn fly *Haematobia irritans*, *Himar1* is a member of the *Tc1/mariner* superfamily of transposable elements (27, 40, 55, 62). *Himar1*-based transposon systems provide an alternative to the most frequently used system in *L. monocytogenes*, a Tn*917* derivative (4). Tn*917*-LTV3 is considerably larger in size (22 kb versus 1.4 kb) and has a relatively low transposition efficiency, a high rate of delivery vector retention, and a tendency for insertional "hot spots" (4, 6, 19). In comparison, the *Himar1*-based transposon system provides several distinct advantages. Transposition requires no additional factor other than the cognate transposase, and similar systems have been shown to be effective in multiple bacterial species, both gram-negative and gram-positive (40, 64). Additionally, *mariner* elements have a low site specificity—the dinucleotide TA—an element common in *L. monocytogenes* (average GC content of 39%) (21, 40).

The increased genomic coverage of *Himar1* transposon-based libraries (both within and between genes) has also facilitated the ease and resolution of negative-selection screens (65). These screens have proven to be a remarkably useful tool, not only in identifying new virulence factors, but also in characterizing which of these factors are necessary during different stages of an infection (8, 35, 43, 65, 66, 86). Furthermore, these approaches have assisted in assigning function to previously uncharacterized virulence factors by mapping their genetic interactions (35).

Recently, a new *Himar1*-based transposon system became available for use with *L. monocytogenes* (6). This transposon does not contain features optimal for its use in a negative-selection screen. Additionally, there is little control over the complexity of the library generated or over instances of clones with multiple transposon insertions. Therefore, we constructed a new *Himar1* system for *L. monocytogenes* based on a different strategy of transposon delivery, one that minimizes the potential for multiple transposition events within a single chromosome and that allows control over the complexity of a library. The new transposon also includes elements that allow us to take advantage of microarray technologies in order to perform negative-selection screens.

Among the factors identified in the screen that lead to a hypohemolytic phenotype was *prsA2*. A peptidyl-prolyl extracytoplasmic *cis/trans* isomerase, PrsA2 has previously been shown to contribute to *L. monocytogenes* virulence, although the precise mechanism remains unknown (9, 52, 56). Furthermore, previous work found that *prsA2* is upregulated upon PrfA activation and preceded by a putative PrfA box, suggesting that *prsA2* is directly regulated by PrfA (9, 52, 56). Here we demonstrate that PrsA2 is critical for virulence and contributes to the secretion and activity of LLO and the activity PC-PLC but is not under direct PrfA control. Additionally, PrsA2 contributes to flagellum-based motility, an aspect of the bacterium's life cycle separate from infection. These data suggest that PrsA2 plays a broader physiological role than previously appreciated.

MATERIALS AND METHODS

Bacterial strains, growth media, and reagents. The bacterial strains used in this study are listed in Table 1. All *Escherichia coli* strains were grown in Luria-Bertani (LB) medium. All strains of *L. monocytogenes* were grown in either brain heart infusion (BHI; Difco, Detroit, MI) medium, LB medium, or LB medium supplemented with 25 mM glucose-1-phosphate and 0.2% activated charcoal, with the pH adjusted to 7.3 with 50 mM MOPS (morpholinepropanesulfonic acid) (LB-G1P) as indicated below. All bacterial stocks were stored at −80°C in BHI supplemented with 50% glycerol. Murine L2 fibroblasts were passaged in Dulbecco modified Eagle medium with high glucose (Gibco/Invitrogen, Carlsbad, CA) supplemented with 1% sodium pyruvate, 1% L-glutamine, and 10% fetal bovine serum (GemCell, West Sacramento, CA) at 37°C with 5% CO_2. The following antibiotics were used as indicated at the indicated concentrations: erythromycin (EM), 2 μg/ml; lincomycin (LM), 25 μg/ml; streptomycin, 200 μg/ml; chloramphenicol (CM), 7.5 to 20 μg/ml; and gentamicin (GM), 10 μg/ml (Sigma-Aldrich, St. Louis, MO). All restriction enzymes, T4 DNA ligase, *Taq* DNA polymerase, VentR DNA polymerase, and respective buffers were obtained from New England Biolabs (NEB; Beverly, MA).

pJZ037 construction. The plasmids and primers used to construct pJZ037 are listed in Table 1. The transposon was constructed in pUC19. Using the vector phiMycoMarT7 (65) as a PCR template, primer pair 112 and 24 and pair 29 and 26 were used to amplify the 5′ and 3′ ends, respectively, of this transposon, which included the TA insertion site, the inverted repeat, and the T7 promoter oriented outward (65). Overhangs included in primers 24 and 29 contained a multiple-cloning site consisting of SmaI, KpnI, PstI, the trinucleotide AAA, SpeI, and XhoI.

The transposon backbone was ligated into pUC19 in a three-way ligation to generate pJZ025 using the PstI sites in primers 24 and 29, a SalI site incorporated by primer 112, and a HindIII site incorporated by primer 26. Primers 30 and 31 amplified the Tn*917* ribosomal methyltransferase gene from pLTV3 (4) and ligated it into the transposon backbone at the PstI and SpeI sites to generate pJZ029.

The transposase and its promoter were also assembled in pUC19. To increase the stability of the transposase transcript, the 5′ untranslated region (5′UTR) of *hly* (lmo0202) was first fused upstream of the hyperactive C9 transposase (39). Primers 113 and 114 were used to amplify the transposase; primer 113 contained a 64-bp overhang that included the 51-bp constitutive hyper-*Pspac* promoter [*Pspac*(hy)] (59, 67, 73), and a BamHI site; and primer 114 included a SalI and a HindIII site. This product was ligated into pUC19 using the BamHI and HindIII sites, resulting in pJZ026.

The transposon was digested out of pJZ029 with BamHI and ligated into pJZ026 to generate pJZ032. The inclusion of the 5′UTR of *hly* upstream of the transposase, however, prevented plasmid curing. Therefore, this copy of the transposase was digested out of pJZ032 with EagI and HindIII and replaced with a copy of the transposase generated by primer 134 and primer 114 (which removed the 5′UTR), resulting in pJZ039. The transposon and transposase were digested out of pJZ039 with SalI and ligated into the gram-positive suicide vector pKSV7 to generate pJZ037 (Fig. 1A) (75).

Generation of libraries. Electrocompetent *L. monocytogenes* organisms were prepared as previously described (54), with the exception that vegetable peptone broth (Remel, Lenexa, KS) was used instead of BHI to increase electroporation efficiency. Approximately 1 μg of pJZ037 was used to electroporate each 50-μl aliquot of electrocompetent cells. Bacteria were recovered in 1 ml of vegetable peptone broth-0.5 M sucrose and plated over approximately 10 100-mm BHI EM-LM agar plates. Plates were incubated for 48 h at 30°C (the permissive temperature) and then replica plated onto BHI EM-LM agar plates and incubated overnight at 41.5°C (the nonpermissive temperature) to cure the plasmid. Colonies were then counted, scraped, and resuspended in BHI-40% glycerol for storage at −80°C.

To test for plasmid retention, 10-fold serial dilutions were prepared from a small frozen aliquot of the library. Each dilution was plated on a BHI plate containing EM (the resistance marker carried by the transposon) and on a plate containing CM (the resistance marker carried by the delivery vector).

TABLE 1. Oligonucleotide primers, plasmids, and strains used in this study

Primer, plasmid, or strain	Sequence (5′→3′) or description[a]	Restriction enzyme(s)	Reference and/or source(s)
Primers			
112	AAAGTCGACTAACAGGTTGGCTGATAAGTCCC	SalI	
24	AAACTGCAGGTACCCGGGTTCCAGTTTGTAATACGACTCAC	SmaI, KpnI, PstI	
29	AAACTGCAGAAAACTAGTCTCGAGTGGGGTACGCGTAATACGACTC	PstI, SpeI, XhoI	
26	AAAAAGCTTGGATCCTAACAGGTTGGCTGATAAGTCCC	BamHI, HindIII	
30	AAACTGCAGCTAAAGTTATGGAAATAAGACTTAG	PstI	
31	AAAACTAGTATTCAAATTTATCCTTATTGTACAAA	SpeI	
113	AAAGGATCCAATTTTGCAAAAAGTTGTTGACTTTATCTACAAGGTGT GGCATAATGTGTGTCGGCCGATAAAGCAAGCATATAATATTGCGT TTCATC	BamHI, EagI	
114	AAAAAGCTTGTCGACTTATTCAACATAGTTCCCTTCAAGA	SalI, HindIII	
134	AAACGGCCGATGGAAAAAAAGGAATTTCGTGTTTTG	EagI	
229	AAAGTCGACTGGAACCGGAGAAGAAACGC	SalI	
230	GTGTTTTTTAGTGCTTATTTAGATCCAAGAATTAATTTCTTCTTCAT		
231	ATGAAGAAGAAATTAATTCTTGGATCTAAATAAGCACTAAAAAACAC		
232	AAACTGCAGGAAACAGTAGACCTATTCTTGC	PstI	
241	AACGGCCGTTTCACACCAATCGGACATTCC	EagI	
242	AACGGCCGACCATAAGAATATCATTAAATTTCTTTC	EagI	
243	AACGGCCGATGAAGAAGAAATTAATTCTTGGAC	EagI	
249	AAAGTCGACTAAAGTACTAAAACATACAAAACCG	SalI	
MSPY5	ACTACGCACCGGACGAGACGTAGCGTC		79
MSPY3	p-CGGACGCTACGTCCGTGTTGTCGGTCCTG		79
Plasmids			
pBADC9			39
phiMycoMarT7			65
pUC19			Invitrogen
pLTV3			4
pKSV7			75
pPL2			42
pJZ025			This study
pJZ026			This study
pJZ029			This study
pJZ032			This study
pJZ037			This study
pJZ039			This study
pJZ064			This study
pJZ065			This study
pJZ066			This study
L. monocytogenes strains			
10403S	WT		3
DP-L5539	*Himar1* transposon generated library, strain 10403S		This study
DP-L5558	Transposon insertion into lmo0964		This study
DP-L5566	Transposon insertion into lmo1268		This study
DP-L5570	Transposon insertion into lmo1401		This study
DP-L5575	Transposon insertion into lmo1609		This study
DP-L5577	Transposon insertion into lmo1695		This study
DP-L5580	Transposon insertion into lmo1821		This study
DP-L5596	Transposon insertion into lmo2219		This study
DP-L5600	Transposon insertion into lmo2460		This study
DP-L5601	10403S Δ*prsA*(*29-291*)		This study
DP-L5602	10403S Δ*prsA*(*29-291*) $tRNA^{Arg}$::pPL2 with construct 1		This study
DP-L5603	10403S Δ*prsA*(*29-291*) $tRNA^{Arg}$::pPL2 with construct 2		This study
DP-L5604	10403S Δ*prsA*(*29-291*) $tRNA^{Arg}$::pPL2 with construct 3		This study
DP-L5605	10403S Δ*prsA*(*29-291*) $tRNA^{Arg}$::pPL2		This study
DP-L2161	10403S Δ*hly*		33
DP-L5606	10403S Δ*hly prsA2*::*Himar1*		This study
DP-L4057	10403S LLO_{S44A}		22
DP-L5607	10403S LLO_{S44A} *prsA2*::*Himar1*		This study
DP-L4361	10403S LLO_{FLAG}		This study
DP-L5608	10403S LLO_{FLAG} *prsA2*::*Himar1*		This study
DP-L861	SLCC-5764		44
DP-L5609	SLCC-5764 *prsA2*::*Himar1*		This study
DP-L1935	10403S Δ*plcB*		74
DP-L4650	10403S Δ*flaA*		85
DP-L4317	10403S Δ*prfA*		H. Shen and J. F. Miller; 10
DP-L3481	10403S LLO_{His6}		20
DP-L5633	10403S LLO_{His6} *prsA2*::*Himar1*		This study

[a] Underlining indicates restriction enzyme sites. Δ*prsA*(*29-291*), the deletion in *prsA* resulting in the removal of amino acids 29 to 291; p-, 5′-phosphate.

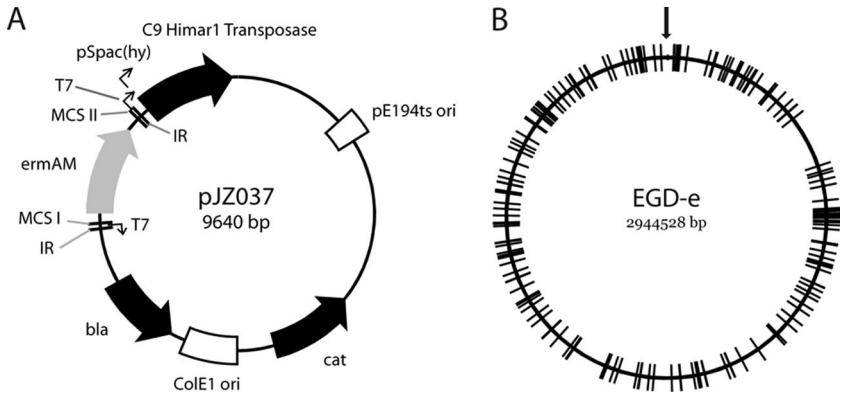

FIG. 1. *Himar1*-based transposon delivery system for *L. monocytogenes*. (A) The vector pJZ037 contains the following features: the ColE1 origin of replication and a β-lactamase resistance gene (*bla*) for propagation in *E. coli*; a gram-positive, temperature-sensitive origin of replication (pE194ts ori) and CM resistance gene (*cat*) for plasmid curing in *L. monocytogenes* (75); the hyperactive C9 variant of the *Himar1* transposase (39) under the control of the pSpac(hy) promoter (59); and the transposon containing the EM resistance gene (*ermAM*) (4) for transposon insertion selection flanked on both sides by T7 promoters oriented outwards for negative-selection screens and the inverted repeats (65). Two multiple-cloning sites (MCS I and MCS II) flank the EM resistance gene. (B) Locations of 197 insertions mapped onto the *L. monocytogenes* EGD-e chromosome. Each line represents a different feature (ORF, intergenic region, or rRNA, etc.). The insertions were obtained from multiple ongoing screens in our lab searching for different phenotypes. The downward-pointing arrow marks the origin of replication.

Blood plate screen for hypohemolytic mutants. Swabs from frozen libraries were added to BHI and plated directly onto 1% LB-G1P agar supplemented with 5% defibrinated sheep's blood (HemoStat Laboratories, Dixon, CA) at a concentration of 150 to 200 colonies per 100- by 15-mm plate. Plates were incubated for 48 h at 37°C, and zones of hemolysin were evaluated by eye for both size and extent of translucency. Potential hits were restreaked on BHI agar containing EM and LM to confirm the presence of the transposon and the absence of the plasmid. To confirm the phenotype, both mutant and WT bacteria were grown overnight at 37°C in BHI with aeration and plated on blood agar plates in a 1:1 ratio. Plates were scanned using Adobe Photoshop (Adobe Systems, San Jose, CA).

Identification of transposon insertion sites. Chromosomal DNA of 2-ml overnight cultures of each mutant were extracted using the MasterPure gram-positive DNA purification kit (Epicentre, Madison, WI), and the instructions were followed with the exception that 10 to 15 units of mutanolysin (Sigma) was used for 1 h at 37°C instead of lysozome. A mixture containing 8 pmol/μl of primers MSPY5 and MSPY3 in 1× T4 DNA ligase buffer was boiled for 5 min and allowed to cool to room temperature (79), creating a partially double-stranded "Y-linker." A reaction mixture containing the 2 μg of digested genomic DNA, 2 μl of the Y-linker, and 400 U of T4 DNA ligase was allowed to incubate at 16°C for 12 h before inactivation of the ligase. Approximately one-third of this reaction mixture was used as a template in an initial PCR to enrich for single-stranded DNA fragments containing the transposon insertion. A 20-μl total reaction volume that included a 0.02 mM concentration of the deoxynucleoside triphosphates (Fermentas, Glen Burnie, MD), 1.5 U *Taq* (NEB), 1× ThermoPol buffer, and a 0.1 μM concentration of primer 121 was first incubated at 95°C for 2 min; incubated at 94°C for 1 min, 61°C for 1 min, and 72°C for 1 min for 20 cycles; and then incubated at 72°C for 7 min. An additional 0.2 mM concentration of the deoxynucleoside triphosphates, 7.5 U of *Taq* (and appropriate buffer), and a 1.5 μM final concentration of primer 121 and of primer 99 were added, and the reaction volume increased to 100 μl (total). This mixture was subjected to the conditions described above, except that the cycle number was increased from 20 to 25 and the final extension time was increased from 7 min to 10 min. The entire reaction volume was run out on a 1% agarose gel, visible bands were excised, and the DNA was purified using the QIAquick gel extraction kit (Qiagen, Valencia, CA). One hundred nanograms of DNA was submitted to the UC Berkeley DNA Sequencing Facility with primers 184 and 185 for sequencing.

L2 plaque assays. Plaque assays on murine L2 fibroblasts were performed as previously described (78). Briefly, the optical densities (ODs) of static, overnight 30°C cultures of *L. monocytogenes* were normalized, washed three times in phosphate-buffered saline, and allowed to infect monolayers of L2 cells for 1 h. Cells were washed and overlaid with 3 ml of 0.7% agar and GM. After 3 days at 37°C, an overlay containing 2 ml of 0.7% agar-GM was added, and ~2.5× neutral red (Sigma-Aldrich) was added. Monolayers were stained overnight, and plaque size was evaluated using ImageJ (http://rsbweb.nih.gov/ij/). At least three wells were used per mutant per experiment, and within each experiment the average size of each strain was measured as a percentage of the average size of the WT plaques.

Hemolytic-activity assays. Hemolytic-activity assays were performed as previously described (57, 73), with some modifications. Briefly, 1 ml of a static, overnight, 30°C LB medium culture of *L. monocytogenes* was diluted into 9 ml of LB medium and grown for 5 h at 37°C with aeration. The OD at 600 nm was determined. Twofold dilutions of culture supernatants were activated in assay buffer containing 1× phosphate-buffered saline (Gibco/Invitrogen) and 8.5×10^{-5} M cysteine-HCl (final pH, 5.5; Sigma-Aldrich) at 37°C for 30 min before a 1/10 volume of 5% sheep's blood was added for another 30 min at 37°C. Purified LLO was first adjusted to an initial concentration of 2 μg/ml in assay buffer, before serial dilutions in assay buffer were made. The assay was completed as described above except that the 30-min activation step was not performed. Hemolytic units were defined as the reciprocal of the dilution of culture supernatant that yielded 50% lysis of sheep red blood cells.

Purification of histidine-tagged LLO from *L. monocytogenes*. Ten-milliliter samples of overnight cultures of DP-L3481 (20) and DP-L5633 grown at 37°C in LB medium with aeration were diluted into 1 liter of LB medium and grown for 8 h at 37°C with aeration. Culture supernatants were obtained by centrifugation at 6,000 × *g* for 15 min and purified by Ni-nitrilotriacetic acid affinity chromatography (Qiagen) according to the manufacturer's recommendations. Samples were loaded onto the column using gravity. Columns were washed first with 30 ml of buffer B (70) and then with 30 ml of buffer B with 150 mM imidazole. Bound LLO was eluted with 15 ml of buffer B with 500 mM imidazole. The eluted protein was dialyzed twice in 500 ml of storage buffer (70) at 4°C, at first overnight and then again for 4 h. Toxin was then mixed with 10% (vol/vol) glycerol and stored at −80°C. Prior to analysis, thawed samples were centrifuged at 13,200 × *g* for 10 min at 4°C to remove precipitated protein. Protein concentration was determined by diluting the toxin 1:10 in 6 M guanidine-HCl and 20 mM Na_2PO_4 (pH 6.5) and measuring the absorbance intensity at 280 nm, using the extinction coefficient obtained by primary sequence analysis with the ExPASy ProtParam tool (http://us.expasy.org/tools/protparam.html) (89).

CIs and total-CFU assays. Competitive indices (CIs) and total-CFU assays were performed as previously described (2). A total of 1.0×10^5 CFU/ml of the mutant or, in the case of the CI, a 1:1 ratio of mutant to WT was intravenously injected into the tail vein of 9- to 14-week-old female C57/B6 mice (The Jackson Laboratory, Bar Harbor, ME). To confirm the bacterial load of the injection mixture, dilutions of the input pool were plated onto BHI-streptomycin plates. Livers and spleen were harvested 48 h postinfection and homogenized in 10 ml and 5 ml, respectively, of 0.2% NP-40 (Calbiochem, Darmstadt, Germany). For the CIs, data were obtained for each mutant from at least seven livers and spleens as previously described (2). For the total-CFU assay, five age-matched mice were injected per strain, and the experiment was repeated twice. All animal work was done in accordance with university regulations.

In-frame deletions and complementation. A WT strain carrying an internal deletion of *prsA2* was constructed as previously described (5). Briefly, primer

pairs 229 and 230 and 231 and 232 were used to amplify the regions ~900 bp upstream and downstream of *prsA2*, respectively. These fragments were fused using splice overlap extension PCR and were introduced into the *L. monocytogenes* organisms via allelic exchange using pKSV7 (5, 28). Primers 241, 242, and 243 were each used as the 5′ primer with primer 249 to generate the complementation fragments 1, 2, and 3, respectively (see Fig. 4B). These fragments were ligated into pPL2 to generate pJZ064, pJZ065, and pJZ066, respectively, and incorporated into the *L. monocytogenes* chromosome as previously described (42).

Transductions. Transductions were performed as previously described using the phage U153 (29). Briefly, 10^7 phage grown on the donor strain were incubated with 10^8 recipient bacteria and then transferred to EM-LM-BHI plates. Colonies were visible after 48 h of incubation at 37°C.

Isolation of bacterial, secreted proteins and subsequent analyses. Overnight 37°C shaking cultures of *L. monocytogenes* in LB-G1P were back diluted to an OD at 600 nm of 0.01 in LB-G1P. Cultures were grown for 8 h at 37°C with shaking, and ODs were taken every hour. Approximately 1.2 ml of culture was taken from each sample at 8 h and spun at 13,200 × *g* to pellet the bacteria. Supernatants were removed and stored at −80°C. In order to normalize for protein secretion during the entire growth curve, the area under the curve was derived using KaleidaGraph (Synergy Software, Reading, PA). Each sample was normalized to the lowest value in a 1.2-ml total volume. Proteins were precipitated with a final concentration of 10% trichloroacetic acid (TCA) (Calbiochem), washed with ice-cold acetone, and resuspended in 2× sample buffer (Invitrogen) containing 5% β-mercaptoethanol. The same fraction of each sample was run out on a 1.0-mm, 12-well NuPAGE 10% Bis-Tris gel plate (Invitrogen). Gels were either stained using the Novex colloidal-blue staining kit (Invitrogen) or subjected to Western blot analysis. Following Western transfer, blots were probed with a rabbit polyclonal LLO antibody and Alexa-Fluor goat anti-rabbit immunoglobulin G (Molecular Probes, Eugene, OR) or, additionally where noted below, with an anti-FLAG M2 monoclonal antibody (Stratagene, Cedar Creek, TX) and goat anti-mouse IRDye 800CW (LiCor Biosciences, Lincoln, NE) (67). Blots were visualized using the Odyssey infrared imaging system (LiCor).

Assay for egg yolk opacity. Egg yolk agar plates were prepared and assay conditions were performed as previously described (90).

Assay for motility. Overnight 30°C BHI static cultures of *L. monocytogenes* were spotted on semisolid (0.35% [wt/vol] agar) BHI plates and incubated for 24 h and 48 h at 30°C.

RESULTS

Construction of a *Himar1 mariner* transposon delivery system. A *Himar1*-based transposon delivery system, pJZ037, was constructed for use in *L. monocytogenes* (Fig. 1A); the plasmids and primers used are listed in Table 1. To diminish the occurrence of multiple transposon hops within single clones and clonal populations, problems that are associated with a previously constructed *Himar1* system (6, 90; data not shown), as well as to add control over the complexity of the library, the hyperactive C9 variant of the *Himar1* transposase (39) was placed under the control of the constitutive, strong, exogenous promoter *Pspac*(hy) (59, 67, 73), and transposition events were allowed to occur on BHI plates. The transposon contains the Tn*917* ribosomal methyltransferase gene (EM resistance) (4) flanked by the TA insertion sites, the inverted repeats, and T7 promoters oriented outwards from the vector phiMycoMarT7 in order to facilitate negative-selection screens (65). Both elements have been ligated into the gram-positive suicide vector pKSV7 (75).

Evaluation of the new *Himar1* transposon delivery vector. A library of approximately 30,000 distinct insertion mutants was generated using pJZ037. Based on the number of colonies that were CM resistant (the drug marker carried by the delivery vector) compared to the number that were EM resistant, approximately 99% of the clones in the library had transposon insertions and had lost the delivery plasmid. Twenty randomly selected clones were subjected to analysis via Southern blotting. All 20 clones examined contained a single transposon insertion, and each insertion site appeared unique (data not shown).

As an additional measure of library coverage, transposon insertion mutants isolated from three screens in the lab (two unrelated to the one described in this report), with focus on different phenotypes, were mapped onto the assembled genome of *L. monocytogenes* EGD-e (Fig. 1B). Each site represents an insertion into a different feature (open reading frame [ORF] or intragenic region, etc.). This map includes 197 insertions and covers most of the genome, with only minimal lengths of sequence lacking insertions. The largest of these regions covers a length of approximately 160,000 bp, a portion of the chromosome from lmo401 to lmo0539, perhaps indicating the presence of many essential genes.

An in vivo negative-selection screen was also performed similarly to previously described screens (66, 86). Preliminary analysis of the data revealed that genes within the PrfA regulon were negatively selected for growth in vivo in mice and guinea pigs (J. Leber, J. D. Sauer, J. Zemansky, and D. A. Portnoy, unpublished observations; C. Cooke, S. Wong, and A. Bakardjiev, unpublished observations).

A transposon mutant screen for *L. monocytogenes* genes involved in the production or activity of LLO. To identify determinants that govern LLO production, activity, or secretion, a screen for hypohemolytic transposon mutants on sheep's blood agar was performed. Approximately 50,000 transposon insertions were screened on 1% LB-G1P agar plates containing 5% defibrinated sheep's blood. The inclusion of the LB-G1P increased the expression of PrfA-regulated genes, including *hly*, and therefore enhanced visual resolution (61). Mutants were visually scored for a decrease in the size of and/or the opacity of the zone of hemolysis, with avoidance of small colonies. Two hundred fifty-one mutants were initially chosen, and 193 were confirmed and sequenced. The precise insertion site of the transposon was determined for 162 of these mutants, 111 of which were unique. These mutants mapped to a total of 57 unique features, including genes and intergenic regions (Table 2). Multiple *hly* mutants, representing 14 distinct transposon insertion sites, were isolated. Of the remaining 31 mutants, the insertion site was determined to within approximately 200 bp. Most of these sites overlapped features already identified; however, six were unique (Table 2). These data suggested that we were approaching saturation, and no additional screening was performed.

Analysis of transposon mutants displaying a hypohemolytic phenotype. The intracellular life cycle of *L. monocytogenes* can be evaluated ex vivo by the capacity of bacteria to form plaques on mouse L2 monolayers. Defects in any component of this life cycle—in particular, LLO-mediated escape from the primary vacuole, escape from the secondary vacuole during cell-to-cell spread, and failure to compartmentalize LLO activity to the phagosome—can influence plaque size and shape. In previous studies, small-plaque mutants of *L. monocytogenes* invariably had in vivo defects (78). To identify those mutants isolated from our initial screen likely to have in vivo relevance, the average plaque sizes of 51 transposon insertion mutants with the greatest observed hemolytic defect were evaluated (Table 2). Eight mutants consistently developed smaller plaques than

TABLE 2. Unique transposon insertions producing a hypohemolytic phenotype, including those with a precisely mapped site

Strain	Transposon insertion(s)	Gene name[a]	Annotation[a]	Blood plate phenotype[b]	Relative plaque size range (%)[c]
DP-L5540	lmo0027		Similar to PTS system, beta-glucoside-specific enzyme IIABC	-	80–100
DP-L5541	lmo0031		LacI family transcription regulator	-	ND
DP-L5542	lmo0134, lmo0135			-	80–100
DP-L5543	lmo0175, lmo0176			-	80–100
DP-L5544	lmo0201, lmo0202			----	80–100
DP-L5545	lmo0202	*hly*	Listeriolysin O	----	ND
DP-L5547	lmo0223	*cysK*	Similar to cysteine synthase	-	80–100
DP-L5548	lmo0234		Similar to *B. subtilis* YacL	-	80–100
DP-L5550	lmo0279		Similar to anaerobic ribonucleoside triphosphate reductase	-	80–100
DP-L5551	lmo0352		Similar to regulatory proteins (DeoR family)	--	80–100
DP-L5552	lmo0669		Similar to oxidoreductase	-	80–100
DP-L5553	lmo0734		Similar to transcriptional regulator (LacI family)	-	ND
DP-L5554	lmo0785		Similar to transcriptional regulator (NifA/NtrC family)	-	80–100
DP-L5555	lmo0813		Similar to fructokinases	-	80–100
DP-L5556	lmo0821			---	80–100
DP-L5557	lmo0833		Similar to transcriptional regulator	-	80–100
DP-L5558	lmo0964		Similar to *B. subtilis* YjbH	----	See Table 3
DP-L5559	lmo0964, lmo0965			-	80–100
DP-L5561	lmo1017		Similar to phosphotransferase system glucose-specific enzyme IIA	-	80–100
DP-L5562	lmo1079		Similar to *B. subtilis* YfhO	-	80–100
DP-L5563	lmo1254		Similar to alpha,alpha-phosphotrehalase	--	80–100
DP-L5564	lmo1255		Similar to PTS system, trehalose-specific enzyme IIBC	-	80–100
DP-L5566	lmo1268	*clpX*	ATP-dependent protease, ATP-binding subunit	-	See Table 3
DP-L5568	lmo1329	*ribC*	Similar to riboflavin kinase and FAD synthase	-	80–100
DP-L5569	lmo1354		Similar to aminopeptidase P	-	ND
DP-L5570	lmo1401			--	See Table 3
DP-L5571	lmo1475	*hrcA*	Heat-inducible transcription repressor	-	80–100
DP-L5572	lmo1514, lmo1515			-	80–100
DP-L5573	lmo1515			-	80–100
DP-L5574	lmo1575			--	See Table 3
DP-L5575	lmo1609		Similar to thioredoxin	-	80–100
DP-L5576	lmo1616			-	80–100
DP-L5577	lmo1695	*mprF*		-	60–80
DP-L5578	lmo1772	*purC*	Phosphoribosylaminoimidazole-succinocarboxamide synthase	-	80–100
DP-L5579	lmo1814			--	80–100
DP-L5580	lmo1821	*prpC*	Similar to putative phosphoprotein phosphatase	--	See Table 3
DP-L5581	lmo1829		Similar to fibronectin binding proteins	-	80–100
DP-L5582	lmo1878		Manganese transport transcriptional regulator	-	80–100
DP-L5583	lmo1922			-	80–100
DP-L5584	lmo1952, lmo1953			--	80–100
DP-L5586	lmo1954	*drm*	Similar to phosphopentomutase	--	80–100
DP-L5587	lmo1974		Similar to transcription regulators (GntR family)	-	80–100
DP-L5590	lmo2055			-	ND
DP-L5591	lmo2072, lmo2073			-	80–100
DP-L5592	lmo2103, lmo2104			--	80–100
DP-L5593	lmo2110		Similar to mannnose-6 phosphate isomerase	-	80–100
DP-L5594	lmo2203		Similar to *N*-acetylmuramoyl-L-alanine amidase and to internalin B	-	80–100
DP-L5595	lmo2217			-	ND
DP-L5596	lmo2219	*prsA2*	Similar to posttranslocation molecular chaperone	--	See Table 3
DP-L5597	lmo2230		Similar to arsenate reductase	--	80–100
DP-L5598	lmo2361			-	80–100
DP-L5599	lmo2376		Similar to peptidyl-prolyl *cis*/*trans* isomerase	--	ND
DP-L5636	lmo2460		Similar to *B. subtilis* CggR hypothetical transcriptional regulator	-	60–80
DP-L5637	lmo2460, lmo2461			-	80–100
DP-L5638	lmo2461	*sigL*	RNA polymerase factor sigma-54	-	80–100
DP-L5639	lmo2758	*guaB*	Similar to inosine-monophosphate dehydrogenase	-	80–100
DP-L5604	lmo2770		Bifunctional glutamate-cysteine ligase/glutathione synthetase	-	ND
DP-L5546[d]	lmo0202, lmo0203			-	ND
DP-L5565[d]	lmo1255, lmo1256			---	ND
DP-L5567[d]	lmo1295, lmo1296			-	ND
DP-L5585[d]	lmo1953	*pnp*	Similar to purine-nucleoside phosphorylase	--	ND
DP-L5588[d]	lmo2016	*cspB*	Similar to major cold shock protein	---	80–100
DP-L5589[d]	lmo2020	*divIVA*	Similar to cell division initiation protein	-	ND

[a] As identified by NCBI annotation of the *L. monocytogenes* EGD-e genome. PTS, phosphotransferase system; FAD, flavin adenine dinucleotide. Blank spaces indicate that no specific annotation has been assigned.

[b] Qualitative hemolytic defect visually determined by comparison to an adjacent WT colony on a blood agar plate as follows: -, 75%; --, 50%; ---, 25%; ----, 0% of the activity of the WT colony.

[c] Relative to the size of the WT in the L2 fibroblast plaque assay. ND, not done.

[d] The approximate site of the transposon is mapped.

those of the WT: the lmo0964 (similar to *yjbH*), lmo1268 (*clpX*), lmo1401 (similar to *ymdB*), lmo1575 (similar to *ytqI*), lmo1695 (*mprF*), lmo1821 (similar to *prpC*), lmo2219 (*prsA2*), and lmo2460 (similar to *cggR*) mutants (Table 2). Of these genes, only two, lmo1695 and lmo2219, have been characterized for *L. monocytogenes*.

The gene lmo1695 encodes a protein with homology to the multiple-peptide-resistance factor (MprF) of *Staphylococcus aureus*, a membrane protein that catalyzes the transfer of lysine residues to phosphatidylglycerol and is known to have a major role in conferring resistance to antimicrobial peptides (80). This gene was first identified in *L. monocytogenes* as a compo-

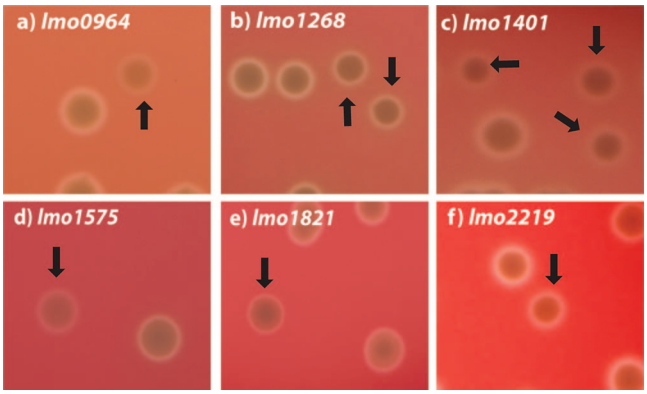

FIG. 2. Blood plate phenotypes for hypohemolytic mutants. Wild-type (10403S) bacteria were plated at a 1:1 ratio with the following transposon insertion mutants on LB-G1P agar containing 5% defibrinated sheep's blood: the lmo0964 (similar to *yjbH*) mutant (A), lmo1268 (*clpX*) mutant (B), lmo1401 (similar to *ymdb*) mutant (C), lmo1575 (similar to *ytqI*) mutant (D), lmo1821 (similar to *prpC*) mutant (E), and lmo2219 (*prsA2*) mutant (F). Arrows denote mutant colonies.

nent of the VirR regulon, and bacteria lacking the response regulator VirR have a reduced ability to colonize and persist in the livers and spleens of infected mice (49). *L. monocytogenes mprF* mutants are attenuated in virulence in mice and have an increased susceptibility to certain cationic antimicrobial peptides (80). Although no study has identified a relationship between LLO secretion and MprF, we eliminated this gene from further analysis, as its role in virulence has already been explored (80) and we suspect that the role of *mprF* on LLO activity is indirect.

The gene lmo2219 is one of two genes in *L. monocytogenes* that encodes a protein with significant homology to the extracytoplasmic lipoprotein chaperone peptidyl-prolyl isomerase PrsA from *Bacillus subtilis*. An essential protein in *B. subtilis*, PrsA contributes to the folding of proteins following Sec-mediated translocation (9, 31, 37, 52, 56). Annotated as *prsA2* (compared to *prsA1* and lmo1444) (56), lmo2219 was first identified as a putative virulence factor in a transcriptome analysis of genes differentially regulated by PrfA; the gene was upregulated under conditions in which PrfA was upregulated, and a putative PrfA binding site was identified upstream of the gene (52). PrsA2 transcript levels were also found to be upregulated during intracellular growth (9), and a proteomics approach found that PrsA2 secretion levels were increased upon PrfA activation (56). These studies also found that *L. monocytogenes prsA2* mutants have a plaquing defect (9, 56), an intracellular growth defect in P388D1 murine macrophage-like cells (9), and a decreased ability to replicate in the livers and spleens of infected mice (56). Speculation that PrsA2 contributes to the folding of extracellular virulence factors remains (9, 56). Given the possibility that one of these substrates could be LLO, we continued characterizing this mutant (see below).

Of the remaining mutations leading to plaque defects, none in *L. monocytogenes* have been characterized. Based on a BLAST search of the *B. subtilis* strain 168 genome (http://www.ncbi.nlm.nih.gov/), the gene lmo0964 is similar to *yjbH* (37% identity, 57% similarity), a gene that confers resistance to nitrosative stress (63). YjbH also plays a role in regulating the response to disulfide stress by acting as a negative effector of the transcriptional regulator Spx (41). Upon disulfide stress, Spx induces the transcription of genes that maintain thiol-redox homeostasis (53). Interestingly, mutants with null mutations in *clpX* and *clpP*, the genes encoding the ATP-powered AAA+ protease ClpXP, have the same phenotype as *yjbH* mutants. A model wherein YjbH facilitates the recognition and degradation of Spx by ClpXP was proposed (41). Consistent with these findings, a transposon insertion in lmo1268, the *L. monocytogenes clpX* gene, was also identified. This mutant has a blood plate phenotype and plaque defect similar to those of the lmo0964 mutant (Fig. 2; Table 3).

The gene lmo1821 codes for a protein similar to the *B. subtilis* protein phosphatase PrpC (49% identity, 67% similarity). In both *L. monocytogenes* and *B. subtilis*, *prpC* is directly upstream of the eukaryotic-type serine/threonine kinase *prkC*; the genes are cotranscribed and appear to have opposing physiological roles during stationary-phase growth and biofilm and spore formation (16, 48). Consistent with its plaque defect, PrkC homologs have been shown to contribute to the virulence of *Enterococcus faecalis*, *Streptococcus pneumoniae*, *Streptococcus agalactiae*, and *Streptococcus pyogenes* (15, 32, 38, 60).

Little is known about the remaining genes. The gene lmo1401 encodes a protein similar to *B. subtilis* YmdB (65% identity, 80% similarity) and contains a putative metallo-phosphoesterase domain. The gene lmo1575 encodes a protein similar to *B. subtilis* YtqI (55% identity, 72% similarity), a protein shown to have both oligoribonuclease and pAp-phosphatase activity [the conversion of 3′(2′)phosphoadenosine 5′ phosphate to AMP] (51). The gene lmo2460 encodes a protein similar to *B. subtilis* CggR (54% identity, 75% similarity), a repressor of the *gapA* operon, which contains many of the genes necessary for glycolysis (14, 47).

We continued to characterize six mutants: the lmo0964 (similar to *yjbH*), *clpX*, lmo1401 (similar to *ymdB*), lmo1575 (similar to *ytqI*), lmo1821 (similar to *prpC*), and *prsA2* mutants (Fig. 2; Table 3). As with the *mprF* mutant, the lmo2460 (*cggR*) mutant was not examined further as it had a small but reproducible growth defect in broth (G1P medium), making it potentially difficult to separate a specific defect in LLO production or activity from a general metabolic defect. The remaining mutants grew in the same way as the WT (data not shown).

TABLE 3. Plaque sizes of transposon insertion mutants

Transposon insertion in mutant	Gene name	Plaque size (% of WT size)[a]
lmo0964	*yjbH*	51.6 ± 5.3***
lmo1268	*clpX*	61.3 ± 2.7***
lmo1401	*ymdB*	35.1 ± 4.5*
lmo1575	*ytqI*	64.7 ± 5.3**
lmo1821	*prpC*	72.4 ± 3.2***
lmo2219	*prsA2*	16.2 ± 1.3***

[a] Mean plaque sizes of murine L2 fibroblasts infected with transposon insertion mutants ± standard deviations, relative to that of the WT strain (the mean plaque size of the WT strain within each experiment was defined as 100%). Each mutant strain was analyzed in at least three experiments. To test the hypothesis that each mean mutant plaque size differs from 100%, a one-sample two-sided *t* test was performed using R software (http://www.r-project.org/). *, $P < 0.005$; **, $P < 0.001$; ***, $P < 0.0005$.

TABLE 4. Hemolytic activities of culture supernatants and purified protein

Strain or purified protein	Hemolytic activity (%)[a]
Strains	
lmo0964::*Himar1* strain	40.3 ± 10.6**
lmo1268::*Himar1* strain	59.7 ± 17.1*
lmo1401::*Himar1* strain	69.9 ± 3.9**
lmo1575::*Himar1* strain	29.6 ± 2.6***
lmo1821::*Himar1* strain	101.5 ± 14.3
Δ*prsA2* mutant	58.0 ± 13.3*
Δ*prsA2* mutant + construct 2	88.7 ± 10.8
Purified protein *prsA2*::*Himar1* LLO_{His6}	67.2 ± 6.1**

[a] Mean percentages of the hemolytic activities of either culture supernatants or purified protein ± standard deviations, relative to WT activity, from at least four experiments. Statistical analysis was performed as described for Table 3. *, $P < 0.05$; **, $P < 0.005$; ***, $P < 0.0005$.

That each mutant's phenotype was due to the transposon insertion was confirmed by transduction (29) into a WT background followed by comparison of the blood plate phenotypes and plaque defects (data not shown).

To assess defects in either the amount of LLO secreted or the activity of the secreted toxin, the hemolytic activity present in culture supernatants of each mutant was determined. As shown in Table 4, the majority of our mutants have decreased hemolytic activity. The lmo1575 insertion mutant had the greatest defect, with an average of 29.6% of the activity of the WT, followed by mutants with transposon insertions in lmo0964 (40.3%) and lmo1268 (*clpX*) (55.9%), an in-frame deletion of *prsA2* (see below) (57.7%), and a transposon insertion in lmo1401 (69.9%). Interestingly, the lmo1821 (*prpC*) transposon insertion mutant had essentially the same level of hemolytic activity as the WT, indicating that the conditions on the blood agar plate (incubation on solid medium for 48 h) elicited a phenotype different from that after growth in broth culture over 5 h.

Western blotting was also performed to assess LLO secretion levels. Although there were small but reproducible qualitative differences in the amounts of LLO secreted by the mutants compared to that secreted by the WT, these differences were not significantly robust to draw any definitive conclusions (data not shown). It is therefore unclear whether the differences identified in the hemolytic-activity assay are due to subtle secretion defects or due to the activity of the LLO secreted (see Discussion).

In vivo analysis of the plaque mutants. To assess the potential virulence defect of each of our six transposon insertion mutants in vivo, a CI assay (2) was utilized to quantify the potential relative replication defect each mutant has in the livers and spleens of C57BL/6 mice coinfected with WT *L. monocytogenes*. For each transposon mutant, five mice were coinfected with 1.0×10^5 bacteria in an ~1:1 ratio of mutant to WT via intravenous tail vein injection. Livers and spleens were harvested 48 h postinfection, and the ratio of WT to mutant bacteria was assessed (2). The *prsA2* insertion mutant displayed the greatest phenotype, as it was undetectable in our organ homogenates after several hundred colonies were patched, consistent with the previously described virulence defect of this mutant of being greater than 2 logs in the liver and spleen (56). The lmo1401 (*ymdB*) insertion mutant also displayed a significant decrease in bacterial numbers in both the liver and spleen, with median defect rates of 2.0 and 1.1 logs, respectively. Consistent with previous studies of the role of *prpC*/*prkC* in virulence in other gram-positive pathogens (15, 32, 38, 60), the transposon insertion in lmo1821 (*prpC*) had a median defect rate of 2.2 logs in the liver and a median defect rate of 1.1 logs in the spleen. Finally, consistent with our hypothesis that transposon insertions in lmo0964 (*yjbH*) and *clpX* affect the same pathway, the relative decreases in bacterial loads between these two mutants (median defect rates of 1.7 versus 1.6 logs in the liver and 0.6 versus 0.7 log in the spleen) were similar (Fig. 3).

In-frame deletion and complementation of PrsA2. Given that the insertion mutation in *prsA2* had the greatest defect in vivo, combined with data (Fig. 2; Table 4) suggesting a link between PrsA2 and LLO secretion and/or activity, we continued to characterize this gene. Two different transposon insertions into *prsA2* were isolated, one 317 bp from the start site and one 410 bp from this site (Fig. 4A). Although one group of investigators was unable to delete PrsA2 (52), this result—that *prsA2* is dispensable—is consistent with the results of two additional groups who were able to inactivate this gene either by making an in-frame deletion (9) or by inserting a plasmid (56).

Both mutants with transposon insertions in *prsA2* had the same blood plate phenotype and plaque defect (data not shown). For the remainder of this study, the insertion 317 bp downstream from the start of the gene was used. However, to confirm that the observed phenotypes were the result of a disruption of *prsA2* and not due to an unlinked mutation, an in-frame deletion of *prsA2*, resulting in a removal of amino acids 9 to 291 (the protein is 293 amino acids long), was carried out (5). The resulting strain, the Δ*prsA2* mutant, has the same plaque defect as that of the strains with either transposon insertion (Table 5).

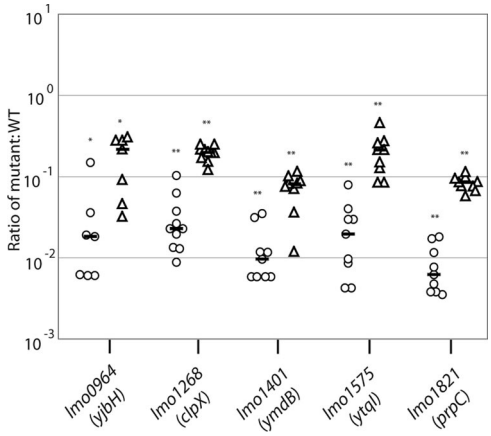

FIG. 3. In vivo defects of transposon insertion mutants as measured by CI. Bacteria were harvested 48 h postinfection from at least seven mice per mutant, and the ratios of mutant to WT bacteria were determined for the liver (○) and spleen (△). All median values are represented by horizontal lines. We performed one-sample Wilcoxon tests on the ratios, using R software (http://www.r-project.org/). Under the null hypothesis of no differences, the mean parameter is assumed to be one. A two-tailed *P* value is reported for each mutant. *, $P < 0.05$; **, $P < 0.005$.

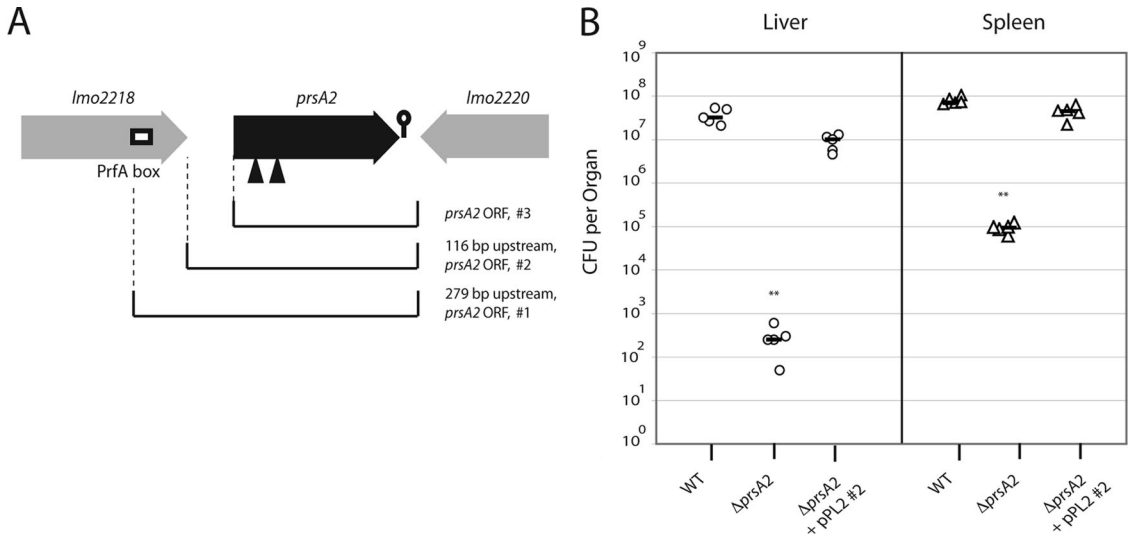

FIG. 4. Virulence of *L. monocytogenes prsA2* mutants. (A) Schematic of the *prsA2* genomic loci and the three different constructs used to complement Δ*prsA2*. Each construct differed at its 5′ end from the others; construct 1 (#1) contained the identified PrfA box, construct 2 (#2) contained the region immediately downstream of lmo2218, and construct 3 (#3) contained just the ORF of *prsA2*. The two triangles below *prsA2* indicate the two transposon mutants isolated in this screen. Stem-loop structures denote transcription terminators. (B) WT, Δ*prsA2*, and Δ*prsA2* strains complemented with construct 2 were analyzed for total bacterial load in the livers (○) and spleens (△) of mice 48 h postinfection. All median values are represented by horizontal lines. Each experiment was repeated. We performed paired Student's *t* tests on the total bacterial load data, using R. Under the null hypothesis of no differences, the mean parameter is assumed to be zero. A two-tailed *P* value is reported for each mutant. **, $P < 0.005$.

To evaluate the in vivo role of *prsA2*, mice were intravenously injected with WT or Δ*prsA2 L. monocytogenes* and livers and spleens were harvested 48 h postinfection to determine total bacterial loads. Consistent with the results of the CI assay for the transposon insertion into *prsA2*, the Δ*prsA2* strain was greater than 5 logs less virulent in the liver and 2.8 logs less virulent in the spleen (Fig. 4B). To further confirm the in vivo role of *prsA2*, we complemented our in-frame deletion of *prsA2* with a chromosomal copy. Previous studies had found an increase in *prsA2* transcript and protein levels upon *prfA* induction, and a putative PrfA box had been identified 206 bp upstream of the start of the *prsA2* ORF (9, 52, 56). However, this location places the start of the promoter 90 bp within the 3′ end of the upstream gene lmo2218. Of the 10 genes confirmed to be directly regulated by PrfA, none has the promoter located within an upstream gene (71).

To test whether the putative PrfA box was dispensable, three different constructs to complement the Δ*prsA2* mutant were designed, each differing at its 5′ end from the others. The first contains the putative PrfA box (construct 1), the second construct contains just the region directly downstream of the 3′ end of the lmo2218 ORF, and a third control construct contains just the ORF of *prsA2* (Fig. 4A). The 3′ end of each construct includes the 131-bp region downstream of *prsA2*, including the terminator sequence (Fig. 4A). Each construct was placed into the integration vector pPL2 (42) and integrated into the chromosome of the Δ*prsA2* strain. As an additional control, an empty pPL2 vector was also integrated into the parent Δ*prsA2* strain.

TABLE 5. Complementation data

Complemented strain	Plaque size (%)[a]
Δ*prsA2* strain	18.2 ± 4.6*
prsA2::*Himar1* strain + construct 1	100.6 ± 5.1
prsA2::*Himar1* strain + construct 2	99.1 ± 2.1
prsA2::*Himar1* strain + construct 3	16.3 ± 3.2
prsA2::*Himar1* strain + empty pPL2 plasmid	17.0 ± 3.4

[a] Mean plaque sizes of murine L2 fibroblasts infected with either the strain with the in-frame deletion of *prsA2* or the *prsA2* transposon insertion mutant complemented with different constructs, relative to the WT plaque size, ± standard deviations. Statistical analysis was performed as described for Table 3. *, $P < 0.005$.

The ability of these constructs to complement the plaque defect of the *prsA2* transposon insertion mutant was analyzed. As expected, both the Δ*prsA2* strain containing just the ORF and the Δ*prsA2* strain with the empty pPL2 vector produced plaques of the same size as those of the transposon insertion mutant and the Δ*prsA2* strain (Table 5). Interestingly, both construct 1 and construct 2 complemented the transposon mutant equally well, suggesting that the PrfA box was dispensable. The ability of the strain containing construct 2 to complement the in-frame deletion in vivo was tested. This construct restored full virulence, as well as complemented the hemolytic activity defect of the Δ*prsA2* culture supernatants (Table 4), again suggesting that the PrfA box is dispensable for *prsA2* expression and activity (Fig. 4B).

Possible role for PrsA2 in folding exported LLO. Western blot analysis of LLO secretion in the Δ*prsA2* mutants revealed an unusual banding pattern: in addition to a major band at approximately 58 kDa (LLO), there were two minor bands at approximately 43 and 41 kDa (Fig. 5A). This laddering pattern is absent in the Δ*prsA2* strain complemented with construct 2.

To confirm that these additional bands were LLO, the transposon insertion mutant was transduced into two different back-

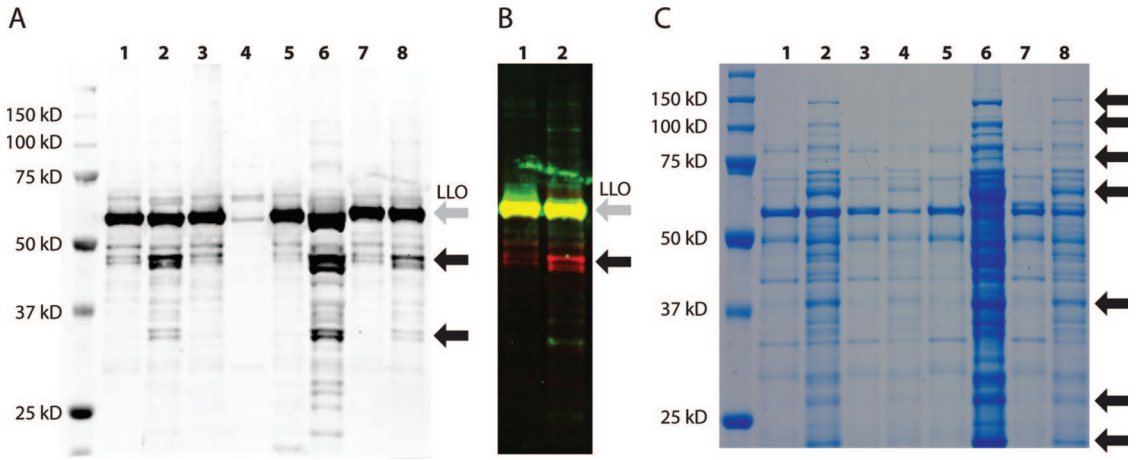

FIG. 5. PrsA2 affects the secretion of LLO. (A) Western blot of secreted proteins probed with a polyclonal anti-LLO antibody from the following bacterial strains: the WT (lane 1), Δ*prsA2* mutant (lane 2), Δ*prsA2* $tRNA^{Arg}$::pPL2 mutant with construct 2 (lane 3), Δ*hly prsA2*::*Himar1* mutant (lane 4), LLO_{S44A} mutant (lane 5), LLO_{S44A} *prsA2*::*Himar1* mutant (lane 6), LLO_{FLAG} strain (lane 7), and LLO_{FLAG} *prsA2*::*Himar1* strain (lane 8). The black arrows indicate the increased presence of the two bands at ~42 kDa and at ~33 kDa in the *prsA2* mutant backgrounds relative to bands in the nonmutated or complemented *prsA2* background. (B) Western blot analysis of the LLO_{FLAG} (lane 1) and LLO_{FLAG} *prsA2*::*Himar1* (lane 2) strains probed with anti-LLO (red) and anti-FLAG (green). The two probes overlap at the major band at 58 kDa but not at ~42 kDa. (C) Colloidal Coomassie blue stain of an SDS-PAGE gel of purified secreted proteins from the same strains as those discussed in panel A. The black arrows indicate the presence of additional bands in the Δ*prsA2* mutant backgrounds (including the Δ*hly* background), as well as molecular masses greater than that of LLO.

grounds: a WT strain containing an in-frame deletion of *hly* (DP-L2161) and a WT strain containing a chromosomal copy of *hly* with the point mutation resulting in S44A (DP-L4057), which relieves the translational inhibition of LLO (LLO_{S44A}). This strain produces and secretes LLO at a constant rate throughout the entire growth cycle of the bacteria (29, 34, 69). These additional strains were subjected to Western blot analysis. In addition to the lack of the major LLO band in the Δ*hly prsA2*::*Himar1* strain, both lower-molecular-weight bands were absent, consistent with the hypothesis that these bands were species of LLO. Additionally, in the LLO_{S44A} *prsA2*::*Himar1* mutant, there was an increase in the size and intensity of the major LLO band as well as in the smaller bands. Furthermore, a smaller set of two bands was visible at approximately 33.5 and 32 kDa; further comparison revealed the presence of these bands in the Δ*prsA2* mutant (Fig. 5A). These results strongly suggested that the additional bands in the *prsA2* mutant backgrounds were lower-molecular-mass species of LLO.

We hypothesized that these additional bands might be degradation products. Bacteria have several mechanisms to refold or degrade misfolded secreted proteins. *B. subtilis*, for example, has several known extracytoplasmic quality control systems, including the serine protease family members HtrA and CWBP52 (82). To investigate this possibility further, a C-terminally epitope-tagged copy of LLO was first employed; LLO contains a cleavable signal sequence at its N terminus (68).

The transposon insertion into *prsA2* was transduced into a WT strain containing a chromosomal copy of LLO with a C-terminal FLAG tag (LLO_{FLAG}) (DP-L4361). The Western blot analysis was then repeated on the LLO_{FLAG} and the *prsA2*::*Himar1* LLO_{FLAG} strains, with probing for both LLO and the FLAG epitope. Consistent with our previous results, when the strain was probed with the anti-LLO antibody, the discrete, smaller bands were of greater intensity in the LLO_{FLAG} *prsA2* transposon mutant. However, these bands did not appear when the strain was probed with the anti-FLAG antibody (Fig. 5B). These results are consistent with our hypothesis that LLO was undergoing C-terminal cleavage in the *prsA2*-disrupted backgrounds.

Purified LLO secreted by the *prsA2* mutant is less active. Both the WT and Δ*prsA2* mutant secreted approximately the same level of full-length LLO, as indicated by Western blot analysis of proteins isolated from culture supernatants (Fig. 5A). We wondered then if the decrease in LLO hemolytic activity of the Δ*prsA2* mutant (Table 4) was due to misfolded full-length LLO. Alternatively, it is possible that the smaller fragments of LLO act in a dominant negative fashion, perhaps by oligomerizing with the full-length toxin but preventing membrane insertion. To address this possibility, full-length LLO was purified from WT or *prsA2*::*Himar1* supernatants and tested for hemolytic activity.

The *prsA2* transposon insertion was transduced into a WT strain of *L. monocytogenes* containing a C-terminally six-histidine-tagged allele of LLO (LLO_{His6}) (DP-L3481) (20). LLO_{His6} was isolated from 8-h culture supernatants from both the WT and *prsA2*::*Himar1* strains by nickel affinity chromatography. The purity of the eluted toxin was confirmed by analysis of the preparation with sodium dodecyl sulfate (SDS)-polyacrylamide gel electrophoresis (PAGE). Additionally, Western blot analysis was used to confirm that the smaller N-terminal fragments of LLO (Fig. 4A) were not present (data not shown). Toxin purified from both the WT and *prsA2*::*Himar1* strains was then diluted appropriately and analyzed for hemolytic activity. The activity of purified, full-length LLO_{His6} isolated from the *prsA2*::*Himar1* strain was 67.2% of the WT's activity, similar to the value obtained for the hemolytic activity obtained the from the Δ*prsA2* culture supernatants (Table 4).

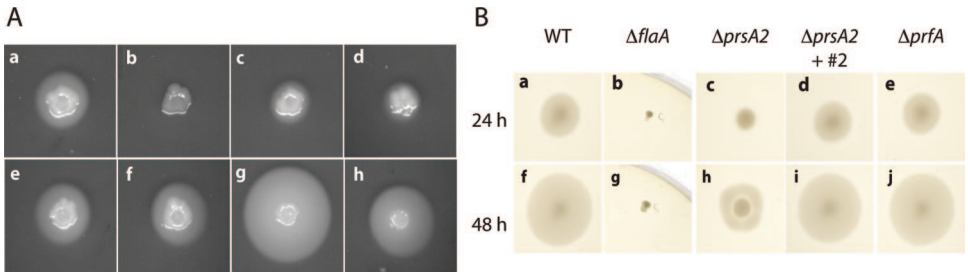

FIG. 6. PrsA2 affects the secretion of additional substrates. (A) PrsA2 mutants affect PC-PLC (lecithinase activity). Overnight cultures grown at 30°C were spotted on 5% (wt/vol) egg yolk LB-G1P plates and grown for 24 h. (a) WT; (b) Δ*plcB* mutant (DP-L1935); (c) Δ*prsA2* mutant; (d) *prsA2*::*Himar1* mutant; (e) Δ*prsA2* $tRNA^{Arg}$::pPL2 mutant with construct 1; (f) Δ*prsA2* $tRNA^{Arg}$::pPL2 mutant with construct 2; (g) SLCC-5764 strain of *L. monocytogenes*; (h) SLCC-5764 (*prsA2*::*Himar1*). (B) PrsA2 mutants affect swarming ability. Overnight cultures grown at 30°C were spotted on 0.35% BHI plates and grown for 24 h (a to e) or 48 h (f to j) at 30°C. (a and f) WT; (b and g) Δ*flaA* mutant (DP-L4650); (c and h) Δ*prsA2* mutant; (d and i) Δ*prsA2* $tRNA^{Arg}$::pPL2 mutant with construct 2; (e and j) Δ*prfA* mutant.

These data are consistent with our hypothesis that PrsA2 is specifically involved in the proper folding of secreted LLO.

Other potential substrates for PrsA2. Examination of a colloidal Coomassie blue-stained SDS-PAGE gel of proteins precipitated from the supernatants of the multiple *prsA2* strains revealed the presence of several bands, both higher in molecular weight than LLO and lower. These bands are not present in either the WT or Δ*prsA2* complemented strains (Fig. 5C).

L. monocytogenes secretes PC-PLC, which contributes to the ability of the bacteria to escape from the primary and secondary vacuoles. The lecithinase activity of PC-PLC, encoded by *plcB*, can be assessed by measuring zones of opacity on an LB agar plate containing egg yolk agar (50, 74, 83). To investigate whether PC-PLC was affected in the *prsA2* mutant, the Δ*prsA2* mutants were tested for lecithinase activity. The Δ*prsA2* strain showed a decreased zone of opacity on egg yolk agar compared to those of both the WT and construct 2-complemented Δ*prsA2* strains (Fig. 6A). To increase the resolution of this assay, the SLCC-5764 (DP-L861) strain of *L. monocytogenes* was utilized. SLCC-5764 contains a *prfA** allele, a dysregulated allele of *prfA* that increases the expression of the PrfA-regulated genes, including *plcB* (26, 44). The *prsA2* transposon insertion was transduced into this strain, which was spotted on an egg yolk agar plate with the parent SLCC-5764 strain. Again, the disruption of *prsA2* caused a visible decrease in the amount of visible lecithinase activity (Fig. 6A).

Given that *prfA* appears to be dispensable for *prsA2* expression, we investigated whether the disruption of *prsA2* causes the disruption of other exported proteins not involved in virulence. *L. monocytogenes* is motile and flagellated at temperatures of 30°C and below but nonmotile at 37°C (24, 25). Given that components of the flagellar machinery are recognized by elements of the immune system, it has been proposed that *L. monocytogenes* actively downregulates the expression of these components upon infection (25). Therefore, to assess the effect of PrsA2 on secretion in a context where PrfA activity is low, the flagellum-based motilities of the mutants were compared.

Cultures of the WT, the Δ*prsA2* mutant, the Δ*prsA2* strain complemented with construct 2, the Δ*flaA* mutant (DP-L4650), and a strain containing in an in-frame deletion of *prfA* (DP-L4317) were all spotted on low-percentage-motility LB agar plates for 24 and 48 h at 30°C. The Δ*prsA2* strain had a smaller swarm pattern than did the WT or the strain complemented with construct 2 (roughly half the size) (Fig. 6B). This defect was, however, considerably smaller than the defect in the Δ*flaA* strain, indicating only a partial loss of swarming ability. This phenotype is consistent with the previous results from the blood and egg yolk agar plates: in all instances, there was only partial loss of activity rather than a complete abrogation. Finally, the Δ*prfA* strain's swarm size was equivalent to that of both the WT and the Δ*prsA2* strain complemented with construct 2, consistent with the complementation results that PrfA appears dispensable for *prsA2* expression and activity.

DISCUSSION

In this study, we have described the construction of a *Himar1*-based transposon system for use in *L. monocytogenes*. This construction decreases many of the issues observed using previous transposon systems in *L. monocytogenes*, specifically, in instances of multiple transposon hops within a single bacterium, clonal populations within a given library (6), and insertion "hot spots" (4). Furthermore, the inclusion of T7 promoters makes negative-selection screens possible. This transposon delivery system is also effective in *Bacillus anthracis* (J. Beaber, J. Zemansky, D. A. Portnoy, R. Calendar, unpublished results).

In order to identify extragenic factors involved in LLO production, activity, or secretion, 50,000 transposon insertions were screened on sheep's blood agar plates for hypohemolytic phenotypes. Critical for virulence, LLO is subject to multiple levels of regulation (68). Given the increased complexity of *Himar1 mariner* transposon mutant libraries, the likelihood of identifying extragenic regulators of LLO, and therefore likely virulence determinants, was increased. Additionally, to our knowledge, this study represents the first published screen for mutants with a hypohemolytic phenotype rather than for those with an ahemolytic phenotype. As a result of the screen, 193 mutants were initially identified as having a hypohemolytic phenotype by visual inspection (Table 2). Plaque assays of murine cells were performed on the 51 mutants with the most discernible visible defect (Table 2).

Given the importance of *hly* in virulence, we expected that a greater fraction of our mutants would exhibit defects escaping from the primary and secondary vacuoles in the ex vivo plaque assay (68). Curiously, of the mutants analyzed, only eight had

repeatable, substantive plaque defects. One possibility for the discrepancy between blood plate phenotype and the lack of an in vivo defect may be that the phenotypes revealed on blood agar might be too subtle to be physiologically relevant. The blood plate assay is very sensitive, as zones of hemolysis are the result of discrete foci of toxin activity occurring over the course of 48 h.

The screen successfully identified both potential novel virulence factors and additional roles for previously described factors; in the eight mutants with both a blood plate phenotype and a plaque defect, six genes—*yjbH*, *clpX*, *ymdB*, *ytqI*, *prpC*, and *cggR*—have not previously been characterized for *L. monocytogenes*. Although the other two genes, *mprF* and *prsA2*, are known to contribute to virulence, a potential relationship between each of these factors and the secretion of LLO has not previously been established (9, 52, 56, 80).

The six characterized mutants displayed a range of defects in the ex vivo plaque assay, the hemolytic-activity assay, and in vivo (Tables 3 and 4; Fig. 3 and 4). The genes *ymdB* (the gene containing the putative metallo-phosphoesterase domain) and *ytqI* (encoding the putative oligoribonuclease) have not been well characterized, and speculating about a potential role in LLO regulation is difficult. Additional work is necessary in order to determine whether the phenotypes of these mutants are the result of a direct relationship with LLO or the PrfA regulon or a more general pleiotropic effect. However, the identification of these genes does suggest that there are as-yet-unidentified factors or pathways that regulate LLO production, secretion, or activity.

More intriguing are the transposon insertions in *yjbH*, *clpX*, *prpC*, and *prsA2*. The association of a strain with a mutation in *prpC*, the phosphatase directly upstream of the eukaryotic-kinase-type serine/threonine kinase, with a virulence defect parallels a similar defect in *prpC prkC* mutants of other gram-positive pathogens (15, 32, 38, 60). Based on BLAST alignments (http://blast.ncbi.nlm.nih.gov/), PrpC is approximately 40% identical and 60% similar to its likely homolog in each of *S. pyogenes* M1 group A streptococci, *S. agalactiae* group B streptococci, *E. faecalis*, and *S. pneumoniae*. Equally intriguing is a recent study that has suggested a role for PrkC in *B. subtilis* in sensing the extracellular environment by binding fragments of peptidoglycan (72). It is therefore tempting to ascribe a direct role for *prpC* and *prkC* in *L. monocytogenes* virulence, possibly by allowing the bacteria to "sense" its environment. However, while mutations in these genes are known to cause changes in the expression of certain virulence factors, they have also been linked to effects on growth, morphology, and cell division and other pleiotropic effects (32, 60). Additional work is required to discern the precise relationship between this kinase/phosphatase pair and members of the PrfA regulon. The reason a difference exists between the phenotype on the blood agar plate (Fig. 2) and the results of the hemolytic-activity assay (Table 4) remains unclear.

yjbH and *clpX* mutants displayed similar blood plate phenotypes, similar hemolytic activities, and similar virulence defects (Fig. 2 and 3; Tables 3 and 4). In *B. subtilis*, their predicted homologs have recently been characterized as regulating the activity of the disulfide stress regulator Spx (41). This transcription factor is responsible for maintaining thiol-redox homeostasis (41, 53), and it is tempting to speculate that the *L. monocytogenes spx* (lmo2191) gene product may answer one of the long-standing questions regarding the toxin. The cholesterol-dependent cytolysins, including LLO, are also known as the "thiol-activated" cytolysins due to the presence of a conserved cysteine residue (76). Crude preparations of these toxins are readily oxidized and require the addition of a reducing agent to reverse the effects. However, this effect diminishes as the purity of the preparation increases, and mutating the cysteine to an alanine does not eliminate LLO hemolytic activity (58). One possible explanation for the conservation of this cysteine residue is that it serves a regulatory role and may be the target site of some external molecule. Perhaps *L. monocytogenes* Spx controls a factor that binds to this residue, sequestering activity. YjbH and/or ClpX would then work to limit the repression by Spx. Consistent with this hypothesis, a transposon insertion into a gene encoding thioredoxin-like protein (lmo1609) was identified (Table 2), although this mutation did not lead to a significant plaque defect.

Most interesting was our finding that a transposon insertion into *prsA2* affected LLO secretion and activity. There was a distinct blood plate phenotype and plaque defect for this mutant (Fig. 2; Table 3). Furthermore, Δ*prsA2* culture supernatant and purified, full-length LLO from a strain containing a transposon in *prsA2* had similar decreased levels of hemolytic activity relative to WT levels (Table 4). Finally, Western blot analysis revealed that while the total levels of LLO exported into the supernatant were similar to WT levels, there were additional lower-molecular-weight species of the toxin (Fig. 5A). The amounts of these species decreased in the complemented strains and drastically increased in a strain of *L. monocytogenes* that overproduced LLO (Fig. 5A). These additional bands did not stain with an anti-FLAG antibody when they were purified from a *prsA2* mutant expressing LLO_{FLAG}, indicating C-terminal cleavage (Fig. 5B). These results strongly suggested that PrsA2 contributes to the proper folding of extracytoplasmic LLO.

Given the additional results that strains lacking PrsA2 have diminished lecithinase activity and a diminished ability to swarm, it is likely that PrsA2 contributes to the folding of several other exported proteins. We therefore hypothesize that the decrease in LLO activity, as well as both the plaque and in vivo defects in *prsA2* mutants, arises as a result of multiple misfolded virulence factors. Our lab is currently investigating this possibility.

Previous studies had identified a link between the expression of *prsA2* and the master virulence transcription factor *prfA*: *prsA2* transcript levels were upregulated during intracellular growth (9) and upregulated in bacteria grown in cytosol-mimicking medium (52), and PrsA2 protein was upregulated in a *prfA** background (56). Given the computationally identified PrfA box upstream of *prsA2*, it was hypothesized that this gene was directly regulated by PrfA (52). However, our results suggest that PrfA does not directly regulate *prsA2* expression: a 116-bp region upstream of *prsA2* lacking the identified PrfA box (Fig. 4A) was sufficient to complement the transposon insertion ex vivo (Table 5) and the in-frame deletion both in the hemolytic-activity assay and in vivo (Fig. 4B). While PrfA may indirectly control *prsA2* expression, there appear to be environmental conditions unassociated with virulence, such as

swarming, under which *prsA2* expression is independent of PrfA (Fig. 6B).

During infection, *L. monocytogenes* undergoes dynamic changes in gene and protein expression (9). This includes the translation of a variety of different PrfA-regulated genes within a short period of time: the genes for internalins (InlA and InlB) to promote uptake into a cell; LLO, the phospholipases C (PI-PLC and PC-PLC), and Mpl to promote phagosome escape; and then ActA to hijack host cell actin (84). The PrfA-regulated genes comprise the most abundant secreted proteins during this transition (71; data not shown).

Interestingly, the effect of the *prsA2* mutants on secreted proteins became more pronounced the more LLO was secreted (Fig. 5C, lanes 2, 4, and 8); the presence of the additional bands noted in the legend of Fig. 5 is most pronounced in the LLO_{S44A} background, followed by the WT background and then the Δ*hly* background. We therefore hypothesize that *L. monocytogenes* PrsA2 is necessary for the bacterium during times of increased export stress. This includes intracellular growth when multiple virulence factors—especially LLO—are produced and secreted in large quantities. Export of these factors occurs through the Sec machinery. Entry and passage through the Sec translocation channel requires substrate proteins to be in a primarily unfolded state (82). Folding at the *trans* side of the membrane is then facilitated by a number of chaperones known as the foldases and include peptidyl-prolyl *cis*/*trans* isomerases (of which PrsA2 is a member) (82). Accumulation of unfolded LLO in the space between the extracytoplasmic side of the membrane and the cell wall in the mutants lacking *prsA2* may lead to either protein degradation or the release of misfolded toxin, resulting in the decrease in hemolysis in vitro (Fig. 2; Table 4) and the virulence defect in vivo (Fig. 4). It is likely that other virulence factors, such as PC-PLC (Fig. 6A), are similarly affected, although whether these factors interact with PrsA2 directly remains unclear. Precedence for this model exists in *B. subtilis*, where the expression of chaperones has been shown to increase in response to extracytoplasmic secretion stress (although those studies were performed with a mutant *prsA* background) (30, 87).

Our hypothesis may explain results from other studies. Gram-positive bacteria have a quality control system for exported factors within the extracytoplasmic space between the cell membrane and peptidoglycan layer (82). One system involves the proteolytic digestion of misfolded proteins by extracytoplasmic proteases, such as the HtrA family of proteases (11, 82). A recent study found that *L. monocytogenes* HtrA levels increased in *prfA** strains (56), and HtrA has been shown to contribute to virulence (77, 88). Our hypothesis is consistent with a model that, under increased export stress, including that experienced upon infection, *L. monocytogenes* upregulates the expression of several factors, including multiple external chaperones such as PrsA2 to manage this stress. These chaperones may prove to be potential targets for therapeutic interventions.

ACKNOWLEDGMENTS

We thank C. Sassetti and E. Rubin for providing the hyperactive C9 *Himar1* transposase and the transducing phage phiMycoMarT7, N. Meyer-Morse for her generous assistance with animal work, N. Wang for her assistance with statistical analyses, R. Calendar for help with transductions, and J. D. Sauer and G. Crimmins for critical reading of the manuscript. We also thank H. Shen and J. Miller for the gift of DP-L4317 and D. Higgins for the gift of *Pspac*(hy) and numerous other vectors and gratefully acknowledge the construction of strain DP-L4361 by A. Decatur.

This research was supported by National Institutes of Health grants AI52154 (H.M.) and AI27655 and P01 AI063302 (D.A.P.). D.A.P. is a Senior Scholar Awardee at the Ellison Medical Foundation. J.H.L. is a Damon Runyon fellow supported by the Damon Runyon Cancer Research Foundation (DRG 1801-04).

REFERENCES

1. **Alouf, J. E.** 2001. Pore-forming bacterial protein toxins: an overview. Curr. Top. Microbiol. Immunol. **257:**1–14.
2. **Auerbuch, V., L. L. Lenz, and D. A. Portnoy.** 2001. Development of a competitive index assay to evaluate the virulence of *Listeria monocytogenes actA* mutants during primary and secondary infection of mice. Infect. Immun. **69:**5953–5957.
3. **Bishop, D. K., and D. J. Hinrichs.** 1987. Adoptive transfer of immunity to Listeria monocytogenes. The influence of in vitro stimulation on lymphocyte subset requirements. J. Immunol. **139:**2005–2009.
4. **Camilli, A., A. Portnoy, and P. Youngman.** 1990. Insertional mutagenesis of *Listeria monocytogenes* with a novel Tn*917* derivative that allows direct cloning of DNA flanking transposon insertions. J. Bacteriol. **172:**3738–3744.
5. **Camilli, A., L. G. Tilney, and D. A. Portnoy.** 1993. Dual roles of plcA in Listeria monocytogenes pathogenesis. Mol. Microbiol. **8:**143–157.
6. **Cao, M., A. P. Bitar, and H. Marquis.** 2007. A *mariner*-based transposition system for *Listeria monocytogenes*. Appl. Environ. Microbiol. **73:**2758–2761.
7. **Chakraborty, T., M. Leimeister-Wachter, E. Domann, M. Hartl, W. Goebel, T. Nichterlein, and S. Notermans.** 1992. Coordinate regulation of virulence genes in *Listeria monocytogenes* requires the product of the *prfA* gene. J. Bacteriol. **174:**568–574.
8. **Chan, K., C. C. Kim, and S. Falkow.** 2005. Microarray-based detection of *Salmonella enterica* serovar Typhimurium transposon mutants that cannot survive in macrophages and mice. Infect. Immun. **73:**5438–5449.
9. **Chatterjee, S. S., H. Hossain, S. Otten, C. Kuenne, K. Kuchmina, S. Machata, E. Domann, T. Chakraborty, and T. Hain.** 2006. Intracellular gene expression profile of *Listeria monocytogenes*. Infect. Immun. **74:**1323–1338.
10. **Cheng, L. W., and D. A. Portnoy.** 2003. Drosophila S2 cells: an alternative infection model for Listeria monocytogenes. Cell Microbiol. **5:**875–885.
11. **Clausen, T., C. Southan, and M. Ehrmann.** 2002. The HtrA family of proteases: implications for protein composition and cell fate. Mol. Cell **10:**443–455.
12. **Cossart, P., M. F. Vicente, J. Mengaud, F. Baquero, J. C. Perez-Diaz, and P. Berche.** 1989. Listeriolysin O is essential for virulence of *Listeria monocytogenes*: direct evidence obtained by gene complementation. Infect. Immun. **57:**3629–3636.
13. **Decatur, A. L., and D. A. Portnoy.** 2000. A PEST-like sequence in listeriolysin O essential for Listeria monocytogenes pathogenicity. Science **290:**992–995.
14. **Doan, T., and S. Aymerich.** 2003. Regulation of the central glycolytic genes in Bacillus subtilis: binding of the repressor CggR to its single DNA target sequence is modulated by fructose-1,6-bisphosphate. Mol. Microbiol. **47:**1709–1721.
15. **Echenique, J., A. Kadioglu, S. Romao, P. W. Andrew, and M. C. Trombe.** 2004. Protein serine/threonine kinase StkP positively controls virulence and competence in *Streptococcus pneumoniae*. Infect. Immun. **72:**2434–2437.
16. **Gaidenko, T. A., T. J. Kim, and C. W. Price.** 2002. The PrpC serine-threonine phosphatase and PrkC kinase have opposing physiological roles in stationary-phase *Bacillus subtilis* cells. J. Bacteriol. **184:**6109–6114.
17. **Gaillard, J. L., P. Berche, J. Mounier, S. Richard, and P. Sansonetti.** 1987. In vitro model of penetration and intracellular growth of *Listeria monocytogenes* in the human enterocyte-like cell line Caco-2. Infect. Immun. **55:**2822–2829.
18. **Gaillard, J. L., P. Berche, and P. Sansonetti.** 1986. Transposon mutagenesis as a tool to study the role of hemolysin in the virulence of *Listeria monocytogenes*. Infect. Immun. **52:**50–55.
19. **Garsin, D. A., J. Urbach, J. C. Huguet-Tapia, J. E. Peters, and F. M. Ausubel.** 2004. Construction of an *Enterococcus faecalis* Tn*917*-mediated-gene-disruption library offers insight into Tn*917* insertion patterns. J. Bacteriol. **186:**7280–7289.
20. **Gedde, M. M., D. E. Higgins, L. G. Tilney, and D. A. Portnoy.** 2000. Role of listeriolysin O in cell-to-cell spread of *Listeria monocytogenes*. Infect. Immun. **68:**999–1003.
21. **Glaser, P., L. Frangeul, C. Buchrieser, C. Rusniok, A. Amend, F. Baquero, P. Berche, H. Bloecker, P. Brandt, T. Chakraborty, A. Charbit, F. Chetouani, E. Couve, A. de Daruvar, P. Dehoux, E. Domann, G. Dominguez-Bernal, E. Duchaud, L. Durant, O. Dussurget, K. D. Entian, H. Fsihi, F. Garcia-del Portillo, P. Garrido, L. Gautier, W. Goebel, N. Gomez-Lopez, T. Hain, J. Hauf, D. Jackson, L. M. Jones, U. Kaerst, J. Kreft, M. Kuhn, F. Kunst, G. Kurapkat, E. Madueno, A. Maitournam, J. M. Vicente, E. Ng, H. Nedjari, G. Nordsiek, S. Novella, B. de Pablos, J. C. Perez-Diaz, R. Purcell, B. Remmel, M. Rose, T. Schlueter, N. Simoes, A. Tierrez, J. A. Vazquez-Boland, H. Voss,**

J. Wehland, and P. Cossart. 2001. Comparative genomics of Listeria species. Science **294:**849–852.
22. **Glomski, I. J., A. L. Decatur, and D. A. Portnoy.** 2003. *Listeria monocytogenes* mutants that fail to compartmentalize listeriolysin O activity are cytotoxic, avirulent, and unable to evade host extracellular defenses. Infect. Immun. **71:**6754–6765.
23. **Glomski, I. J., M. M. Gedde, A. W. Tsang, J. A. Swanson, and D. A. Portnoy.** 2002. The Listeria monocytogenes hemolysin has an acidic pH optimum to compartmentalize activity and prevent damage to infected host cells. J. Cell Biol. **156:**1029–1038.
24. **Gray, M. J., N. E. Freitag, and K. J. Boor.** 2006. How the bacterial pathogen *Listeria monocytogenes* mediates the switch from environmental Dr. Jekyll to pathogenic Mr. Hyde. Infect. Immun. **74:**2505–2512.
25. **Grundling, A., L. S. Burrack, H. G. Bouwer, and D. E. Higgins.** 2004. Listeria monocytogenes regulates flagellar motility gene expression through MogR, a transcriptional repressor required for virulence. Proc. Natl. Acad. Sci. USA **101:**12318–12323.
26. **Grundling, A., M. D. Gonzalez, and D. E. Higgins.** 2003. Requirement of the *Listeria monocytogenes* broad-range phospholipase PC-PLC during infection of human epithelial cells. J. Bacteriol. **185:**6295–6307.
27. **Hartl, D. L., A. R. Lohe, and E. R. Lozovskaya.** 1997. Modern thoughts on an ancyent marinere: function, evolution, regulation. Annu. Rev. Genet. **31:** 337–358.
28. **Ho, S. N., H. D. Hunt, R. M. Horton, J. K. Pullen, and L. R. Pease.** 1989. Site-directed mutagenesis by overlap extension using the polymerase chain reaction. Gene **77:**51–59.
29. **Hodgson, D. A.** 2000. Generalized transduction of serotype 1/2 and serotype 4b strains of Listeria monocytogenes. Mol. Microbiol. **35:**312–323.
30. **Hyyrylainen, H. L., A. Bolhuis, E. Darmon, L. Muukkonen, P. Koski, M. Vitikainen, M. Sarvas, Z. Pragai, S. Bron, J. M. van Dijl, and V. P. Kontinen.** 2001. A novel two-component regulatory system in Bacillus subtilis for the survival of severe secretion stress. Mol. Microbiol. **41:**1159–1172.
31. **Jacobs, M., J. B. Andersen, V. Kontinen, and M. Sarvas.** 1993. Bacillus subtilis PrsA is required in vivo as an extracytoplasmic chaperone for secretion of active enzymes synthesized either with or without pro-sequences. Mol. Microbiol. **8:**957–966.
32. **Jin, H., and V. Pancholi.** 2006. Identification and biochemical characterization of a eukaryotic-type serine/threonine kinase and its cognate phosphatase in Streptococcus pyogenes: their biological functions and substrate identification. J. Mol. Biol. **357:**1351–1372.
33. **Jones, S., and D. A. Portnoy.** 1994. Characterization of *Listeria monocytogenes* pathogenesis in a strain expressing perfringolysin O in place of listeriolysin O. Infect. Immun. **62:**5608–5613.
34. **Jones, S., and D. A. Portnoy.** 1994. Small plaque mutants. Methods Enzymol. **236:**526–531.
35. **Joshi, S. M., A. K. Pandey, N. Capite, S. M. Fortune, E. J. Rubin, and C. M. Sassetti.** 2006. Characterization of mycobacterial virulence genes through genetic interaction mapping. Proc. Natl. Acad. Sci. USA **103:**11760–11765.
36. **Kathariou, S., P. Metz, H. Hof, and W. Goebel.** 1987. Tn*916*-induced mutations in the hemolysin determinant affecting virulence of *Listeria monocytogenes*. J. Bacteriol. **169:**1291–1297.
37. **Kontinen, V. P., and M. Sarvas.** 1993. The PrsA lipoprotein is essential for protein secretion in Bacillus subtilis and sets a limit for high-level secretion. Mol. Microbiol. **8:**727–737.
38. **Kristich, C. J., C. L. Wells, and G. M. Dunny.** 2007. A eukaryotic-type Ser/Thr kinase in Enterococcus faecalis mediates antimicrobial resistance and intestinal persistence. Proc. Natl. Acad. Sci. USA **104:**3508–3513.
39. **Lampe, D. J., B. J. Akerley, E. J. Rubin, J. J. Mekalanos, and H. M. Robertson.** 1999. Hyperactive transposase mutants of the Himar1 mariner transposon. Proc. Natl. Acad. Sci. USA **96:**11428–11433.
40. **Lampe, D. J., M. E. Churchill, and H. M. Robertson.** 1996. A purified mariner transposase is sufficient to mediate transposition in vitro. EMBO J. **15:**5470–5479.
41. **Larsson, J. T., A. Rogstam, and C. von Wachenfeldt.** 2007. YjbH is a novel negative effector of the disulphide stress regulator, Spx, in Bacillus subtilis. Mol. Microbiol. **66:**669–684.
42. **Lauer, P., M. Y. Chow, M. J. Loessner, D. A. Portnoy, and R. Calendar.** 2002. Construction, characterization, and use of two *Listeria monocytogenes* site-specific phage integration vectors. J. Bacteriol. **184:**4177–4186.
43. **Lawley, T. D., K. Chan, L. J. Thompson, C. C. Kim, G. R. Govoni, and D. M. Monack.** 2006. Genome-wide screen for Salmonella genes required for long-term systemic infection of the mouse. PLoS Pathog. **2:**e11.
44. **Leimeister-Wachter, M., W. Goebel, and T. Chakraborty.** 1989. Mutations affecting hemolysin production in Listeria monocytogenes located outside the listeriolysin gene. FEMS Microbiol. Lett. **53:**23–29.
45. **Lety, M. A., C. Frehel, P. Berche, and A. Charbit.** 2002. Critical role of the N-terminal residues of listeriolysin O in phagosomal escape and virulence of Listeria monocytogenes. Mol. Microbiol. **46:**367–379.
46. **Lety, M. A., C. Frehel, I. Dubail, J. L. Beretti, S. Kayal, P. Berche, and A. Charbit.** 2001. Identification of a PEST-like motif in listeriolysin O required for phagosomal escape and for virulence in Listeria monocytogenes. Mol. Microbiol. **39:**1124–1139.
47. **Ludwig, H., G. Homuth, M. Schmalisch, F. M. Dyka, M. Hecker, and J. Stulke.** 2001. Transcription of glycolytic genes and operons in Bacillus subtilis: evidence for the presence of multiple levels of control of the gapA operon. Mol. Microbiol. **41:**409–422.
48. **Madec, E., A. Laszkiewicz, A. Iwanicki, M. Obuchowski, and S. Seror.** 2002. Characterization of a membrane-linked Ser/Thr protein kinase in Bacillus subtilis, implicated in developmental processes. Mol. Microbiol. **46:**571–586.
49. **Mandin, P., H. Fsihi, O. Dussurget, M. Vergassola, E. Milohanic, A. Toledo-Arana, I. Lasa, J. Johansson, and P. Cossart.** 2005. VirR, a response regulator critical for Listeria monocytogenes virulence. Mol. Microbiol. **57:**1367–1380.
50. **Marquis, H., V. Doshi, and D. A. Portnoy.** 1995. The broad-range phospholipase C and a metalloprotease mediate listeriolysin O-independent escape of *Listeria monocytogenes* from a primary vacuole in human epithelial cells. Infect. Immun. **63:**4531–4534.
51. **Mechold, U., G. Fang, S. Ngo, V. Ogryzko, and A. Danchin.** 2007. YtqI from Bacillus subtilis has both oligoribonuclease and pAp-phosphatase activity. Nucleic Acids Res. **35:**4552–4561.
52. **Milohanic, E., P. Glaser, J. Y. Coppee, L. Frangeul, Y. Vega, J. A. Vazquez-Boland, F. Kunst, P. Cossart, and C. Buchrieser.** 2003. Transcriptome analysis of Listeria monocytogenes identifies three groups of genes differently regulated by PrfA. Mol. Microbiol. **47:**1613–1625.
53. **Nakano, S., E. Kuster-Schock, A. D. Grossman, and P. Zuber.** 2003. Spx-dependent global transcriptional control is induced by thiol-specific oxidative stress in Bacillus subtilis. Proc. Natl. Acad. Sci. USA **100:**13603–13608.
54. **Park, S. F., and G. S. Stewart.** 1990. High-efficiency transformation of Listeria monocytogenes by electroporation of penicillin-treated cells. Gene **94:**129–132.
55. **Plasterk, R. H., Z. Izsvak, and Z. Ivics.** 1999. Resident aliens: the Tc1/mariner superfamily of transposable elements. Trends Genet. **15:**326–332.
56. **Port, G. C., and N. E. Freitag.** 2007. Identification of novel *Listeria monocytogenes* secreted virulence factors following mutational activation of the central virulence regulator, PrfA. Infect. Immun. **75:**5886–5897.
57. **Portnoy, D. A., P. S. Jacks, and D. J. Hinrichs.** 1988. Role of hemolysin for the intracellular growth of Listeria monocytogenes. J. Exp. Med. **167:**1459–1471.
58. **Provoda, C. J., and K. D. Lee.** 2000. Bacterial pore-forming hemolysins and their use in the cytosolic delivery of macromolecules. Adv. Drug Deliv. Rev. **41:**209–221.
59. **Quisel, J. D., W. F. Burkholder, and A. D. Grossman.** 2001. In vivo effects of sporulation kinases on mutant Spo0A proteins in *Bacillus subtilis*. J. Bacteriol. **183:**6573–6578.
60. **Rajagopal, L., A. Clancy, and C. E. Rubens.** 2003. A eukaryotic type serine/threonine kinase and phosphatase in Streptococcus agalactiae reversibly phosphorylate an inorganic pyrophosphatase and affect growth, cell segregation, and virulence. J. Biol. Chem. **278:**14429–14441.
61. **Ripio, M. T., K. Brehm, M. Lara, M. Suarez, and J. A. Vazquez-Boland.** 1997. Glucose-1-phosphate utilization by *Listeria monocytogenes* is PrfA dependent and coordinately expressed with virulence factors. J. Bacteriol. **179:**7174–7180.
62. **Robertson, H. M., and D. J. Lampe.** 1995. Recent horizontal transfer of a mariner transposable element among and between Diptera and Neuroptera. Mol. Biol. Evol. **12:**850–862.
63. **Rogstam, A., J. T. Larsson, P. Kjelgaard, and C. von Wachenfeldt.** 2007. Mechanisms of adaptation to nitrosative stress in *Bacillus subtilis*. J. Bacteriol. **189:**3063–3071.
64. **Rubin, E. J., B. J. Akerley, V. N. Novik, D. J. Lampe, R. N. Husson, and J. J. Mekalanos.** 1999. In vivo transposition of mariner-based elements in enteric bacteria and mycobacteria. Proc. Natl. Acad. Sci. USA **96:**1645–1650.
65. **Sassetti, C. M., D. H. Boyd, and E. J. Rubin.** 2001. Comprehensive identification of conditionally essential genes in mycobacteria. Proc. Natl. Acad. Sci. USA **98:**12712–12717.
66. **Sassetti, C. M., D. H. Boyd, and E. J. Rubin.** 2003. Genes required for mycobacterial growth defined by high density mutagenesis. Mol. Microbiol. **48:**77–84.
67. **Schnupf, P., J. Hofmann, J. Norseen, I. J. Glomski, H. Schwartzstein, and A. L. Decatur.** 2006. Regulated translation of listeriolysin O controls virulence of Listeria monocytogenes. Mol. Microbiol. **61:**999–1012.
68. **Schnupf, P., and D. A. Portnoy.** 2007. Listeriolysin O: a phagosome-specific lysin. Microbes Infect. **9:**1176–1187.
69. **Schnupf, P., D. A. Portnoy, and A. L. Decatur.** 2006. Phosphorylation, ubiquitination and degradation of listeriolysin O in mammalian cells: role of the PEST-like sequence. Cell Microbiol. **8:**353–364.
70. **Schuerch, D. W., E. M. Wilson-Kubalek, and R. K. Tweten.** 2005. Molecular basis of listeriolysin O pH dependence. Proc. Natl. Acad. Sci. USA **102:** 12537–12542.
71. **Scortti, M., H. J. Monzo, L. Lacharme-Lora, D. A. Lewis, and J. A. Vazquez-Boland.** 2007. The PrfA virulence regulon. Microbes Infect. **9:**1196–1207.
72. **Shah, I. M., M. H. Laaberki, D. L. Popham, and J. Dworkin.** 2008. A eukaryotic-like Ser/Thr kinase signals bacteria to exit dormancy in response to peptidoglycan fragments. Cell **135:**486–496.
73. **Shen, A., and D. E. Higgins.** 2005. The 5′ untranslated region-mediated

enhancement of intracellular listeriolysin O production is required for Listeria monocytogenes pathogenicity. Mol. Microbiol. **57:**1460–1473.
74. **Smith, G. A., H. Marquis, S. Jones, N. C. Johnston, D. A. Portnoy, and H. Goldfine.** 1995. The two distinct phospholipases C of *Listeria monocytogenes* have overlapping roles in escape from a vacuole and cell-to-cell spread. Infect. Immun. **63:**4231–4237.
75. **Smith, K., and P. Youngman.** 1992. Use of a new integrational vector to investigate compartment-specific expression of the Bacillus subtilis spoIIM gene. Biochimie **74:**705–711.
76. **Smyth, C. J., and J. L. Duncan.** 1978. Thiol-activated (oxygen-labile) cytolysins, p. 129–183. *In* J. Jelaszewicz and T. Wadström (ed.), Bacterial toxins and cell membranes. Academic Press, Inc., New York, NY.
77. **Stack, H. M., R. D. Sleator, M. Bowers, C. Hill, and C. G. Gahan.** 2005. Role for HtrA in stress induction and virulence potential in *Listeria monocytogenes*. Appl. Environ. Microbiol. **71:**4241–4247.
78. **Sun, A. N., A. Camilli, and D. A. Portnoy.** 1990. Isolation of *Listeria monocytogenes* small-plaque mutants defective for intracellular growth and cell-to-cell spread. Infect. Immun. **58:**3770–3778.
79. **Tavazoie, S., and G. M. Church.** 1998. Quantitative whole-genome analysis of DNA-protein interactions by in vivo methylase protection in E. coli. Nat. Biotechnol. **16:**566–571.
80. **Thedieck, K., T. Hain, W. Mohamed, B. J. Tindall, M. Nimtz, T. Chakraborty, J. Wehland, and L. Jansch.** 2006. The MprF protein is required for lysinylation of phospholipids in listerial membranes and confers resistance to cationic antimicrobial peptides (CAMPs) on Listeria monocytogenes. Mol. Microbiol. **62:**1325–1339.
81. **Tilney, L. G., and D. A. Portnoy.** 1989. Actin filaments and the growth, movement, and spread of the intracellular bacterial parasite, Listeria monocytogenes. J. Cell Biol. **109:**1597–1608.
82. **Tjalsma, H., A. Bolhuis, J. D. Jongbloed, S. Bron, and J. M. van Dijl.** 2000. Signal peptide-dependent protein transport in Bacillus subtilis: a genome-based survey of the secretome. Microbiol. Mol. Biol. Rev. **64:**515–547.
83. **Vazquez-Boland, J. A., C. Kocks, S. Dramsi, H. Ohayon, C. Geoffroy, J. Mengaud, and P. Cossart.** 1992. Nucleotide sequence of the lecithinase operon of *Listeria monocytogenes* and possible role of lecithinase in cell-to-cell spread. Infect. Immun. **60:**219–230.
84. **Vazquez-Boland, J. A., M. Kuhn, P. Berche, T. Chakraborty, G. Dominguez-Bernal, W. Goebel, B. Gonzalez-Zorn, J. Wehland, and J. Kreft.** 2001. *Listeria* pathogenesis and molecular virulence determinants. Clin. Microbiol. Rev. **14:**584–640.
85. **Way, S. S., L. J. Thompson, J. E. Lopes, A. M. Hajjar, T. R. Kollmann, N. E. Freitag, and C. B. Wilson.** 2004. Characterization of flagellin expression and its role in Listeria monocytogenes infection and immunity. Cell Microbiol. **6:**235–242.
86. **Weiss, D. S., A. Brotcke, T. Henry, J. J. Margolis, K. Chan, and D. M. Monack.** 2007. In vivo negative selection screen identifies genes required for Francisella virulence. Proc. Natl. Acad. Sci. USA **104:**6037–6042.
87. **Westers, H., L. Westers, E. Darmon, J. M. van Dijl, W. J. Quax, and G. Zanen.** 2006. The CssRS two-component regulatory system controls a general secretion stress response in Bacillus subtilis. FEBS J. **273:**3816–3827.
88. **Wilson, R. L., L. L. Brown, D. Kirkwood-Watts, T. K. Warren, S. A. Lund, D. S. King, K. F. Jones, and D. E. Hruby.** 2006. *Listeria monocytogenes* 10403S HtrA is necessary for resistance to cellular stress and virulence. Infect. Immun. **74:**765–768.
89. **Woodward, J. J., N. I. Martin, and M. A. Marletta.** 2007. An Escherichia coli expression-based method for heme substitution. Nat. Methods **4:**43–45.
90. **Yeung, P. S., N. Zagorski, and H. Marquis.** 2005. The metalloprotease of *Listeria monocytogenes* controls cell wall translocation of the broad-range phospholipase C. J. Bacteriol. **187:**2601–2608.